



Tomas Bata University in Zlín

Centre of Polymer Systems

Doctoral thesis summary

Preparation and characterization of nanocomposite thin films for sensors of organic solvent vapours

Příprava a charakterizace nanokompozitních tenkých vrstev pro senzory par organických rozpouštědel

Author: **Ing. Rostislav Slobodian, Ph.D.**

Study Programme: P3972 Nanotechnology and advanced materials

Study Course: 3942V006 Nanotechnology and advanced materials

Supervisor: prof. Ing. et Ing. Ivo Kuřitka, Ph.D. et Ph.D.

Consultant: Ing. Pavel Urbánek, Ph.D.

Reviewers: doc. Dr. Ing. Vladimír Pavlínek
prof. RNDr. Petr Ponížil, Ph.D.

Zlín, May 2024

© Rostislav Slobodian

Published by **Tomas Bata University in Zlín** in the Edition **Doctoral Thesis Summary**.

The publication was issued in the year 2024.

Key words in Czech: *Mnohostěnné uhlíkové nanotrubicе, grafenové nanodestičky, elastomer, kopolymerní nanokompozit, snímání organických par, nanotechnologie, chemiresistivní plynový senzor, Hansenovy parametry rozpustnosti*

Key words: *Multiwall carbon nanotubes, graphene nanoplatelets, elastomer, copolymer nanocomposites, organic vapour sensing, nanotechnology, chemiresistive gas sensor, Hansen solubility parameter*

Full text of the doctoral thesis is available in the Library of TBU in Zlín.

ISBN 978-80-7678-263-1

Acknowledgement

First, I would like to thank my supervisor, prof. Ivo Kuřitka, PhD. et Ph.D., for the opportunity for doctoral study at the Centre of Polymer Systems (CPS), Tomas Bata University in Zlín. I am thankful for his recruitment after I graduated master's degree and his guidance, advice, knowledge, and support during my Ph.D. study, which was very tough to combine with my work duties. I appreciate the time spent with him was fruitful for me around all kinds of our discussions, and his expertise and ideas were helpful to my research work.

My further gratitude to my main research partner, Robert Olejník, Ph.D., as the supervisor of my master's thesis; he was willing to continue our research and consultations even during my Ph.D. study. Many thanks belong to him for his attitude of helping me with all technical consultations, experimentations, and cooperation in the laboratories. I would also like to extend my gratitude to Jiří Matyáš, Ph.D., for his consultation and cooperation in the field of electrical property measurements.

I'm so glad I could be a member of the Multifunctional nanomaterials research group, which later transformed into Nanomaterials and advanced technology research direction. I am also thankful to all my friends and colleagues I met in this part of life.

Finally, the biggest thanks go to my wife and my family for their love, care, and unstoppable support throughout my life.

Abstract

Nanofillers based on carbon, such as graphene, carbon black, and carbon fibres, are used for composite production. Nowadays, multiwall carbon nanotubes (MWCNTs) are a widely applicable material, mainly in the fields of polymer electronics and sensors. The utilization of carbonaceous nanofillers in various sensors like pressure, deformation, motion, or sensors to detect organic compound vapours is broadly reported. Although their sensitivity is high, most applications for sensing organic vapours suffer from low selectivity. Entangled MWCNTs buckypaper structures may serve as a reference of its kind.

The study presents a new method for preparing nanocomposite-based chemiresistive sensors for volatile organic compounds (VOCs). Ethanol, acetone, toluene, and heptane were selected as representative VOCs differing in polarity and hydrophobicity. The transducing layer of the sensors is made from an elastomeric matrix and carbonaceous nanofillers and deposited on substrates patterned by interdigitated electrodes. Carbon nanotubes were found to be the most suitable of the fillers considered in the first stage of the research. Three nanocomposite materials with comparable resistivity were prepared from elastomeric copolymers with MWCNTs filler. Styrene-isoprene-styrene copolymer, ethylene-octene copolymer, and thermoplastic polyurethane were chosen as the polymer matrices. These samples manifested comparable sensitivity and better selectivity than the previously studied buckypaper. Examples of potential applications such as an integrated electronic device, “electronic nose,” and a sensing microstrip antenna were demonstrated. In the next step of the research, various strategies have been adopted and employed to enhance the performance of the sensors. Spin coating was found to be the best thin film preparation technology, whereas surface plasma treatment did not yield any improvement. The introduction of graphene nanoplatelets (GNPs) as a next filler and styrene-butadiene-styrene copolymer as the next matrix allowed the preparation of VOC sensors with giant response and selectivity. The superior sensor properties were explained using Hansen solubility parameters (HSP). The main advantages of the HSP approach, i.e. simplicity, explanatory and predictive power, were proven also in this study. Moreover, it enables a rational design of new sensors based on solvent–polymer–filler interactions, thus announcing a new class of HSP-based sensors.

Abstrakt

Nanoplňiva na bázi uhlíku, jako jsou grafen, saze a uhlíková vlákna, jsou stále více používaná při výrobě kompozitů. V dnešní době jsou mnohostěnné uhlíkové nanotrubic (MWCNT) široce využívaným materiálem především v oblasti polymerní elektroniky a senzorů. Uvádí se mnoho příkladů použití uhlíkatých nanoplňiv v různých senzorech veličin, jako jsou tlak, deformace, pohyb nebo senzory k detekci par organických sloučenin. Přestože jejich citlivost bývá vysoká, většina aplikací pro snímání koncentrace par organických látek trpí nízkou selektivitou. Zapletené struktury MWCNTs ve formě buckypaperu mohou posloužit jako svého druhu reference.

Předložená studie představuje novou metodu přípravy chemirezistivních senzorů na bázi nanokompozitů pro těkavé organické sloučeniny (VOC). Ethanol, aceton, toluen a heptan byly vybrány jako reprezentativní VOC lišící se polaritou a hydrofobicitou. Převodní vrstva senzorů je vyrobena z elastomerní matrice a uhlíkových nanoplňiv a nanosena na substrátech opatřených interdigitálními elektrodami. Jako nejvhodnější z plňiv uvažovaných v první fázi výzkumu byly sledovány uhlíkové nanotrubic. Z elastomerních kopolymerů a MWCNTs jako plňiva byly připraveny tři nanokompozitní materiály se srovnatelným odporem. Jako polymerní matrice byly zvoleny styren-isopren-styrenový kopolymer, ethylen-oktenový kopolymer a termoplastický polyuretan. Tyto vzorky vykazovaly srovnatelnou citlivost a lepší selektivitu než dříve studovaný buckypaper. Jako příklad možné aplikace bylo demonstrováno integrované elektronické zařízení, „elektronický nos“ a snímací mikropásková anténa. V dalším kroku výzkumu byly přijaty a použity různé strategie pro zlepšení výkonu senzorů. Bylo zjištěno, že rotační potahování je nejlepší technologií přípravy tenkého filmu, zatímco plazmové opracování povrchu nepřineslo žádné zlepšení. Zavedení grafenových nanodesiček (GNP) jako dalšího plňiva a styren-butadien-styrenového kopolymeru jako další matrice umožnilo přípravu VOC senzorů s obrovskou odezvou a selektivitou. Vynikající vlastnosti senzoru byly vysvětleny pomocí Hansenových parametrů rozpustnosti (HSP). Hlavní výhody přístupu HSP, tedy jednoduchost, vypovídací schopnost a prediktivní schopnost, se osvědčily i v této studii. Navíc tento přístup umožňuje racionální návrh nových senzorů založených na interakcích rozpouštědlo–polymer–plňivo, čímž představuje novou třídu senzorů na bázi HSP.

Content

1.	INTRODUCTION	8
1.1	Nanotechnology.....	8
1.2	Polymer nanomaterials	8
2.	POLYMERS	9
2.1	Styrene-isoprene-styrene copolymer (SIS)	9
2.2	Thermoplastic polyurethane (TPU).....	9
2.3	Ethylene-octene-copolymer (EOC).....	10
2.4	Styrene-butadiene-styrene co-polymer (SBS).....	10
3.	CARBON ALLOTROPES	11
3.1	Carbon nanotubes	11
3.2	Graphene.....	11
4.	COMPOSITE / NANOCOMPOSITE	12
4.1	Electrical percolation threshold.....	12
4.2	Advantages of nanocomposites	13
4.3	Preparation of carbon nanotube/polymer composites	13
5.	SENSOR	13
5.1	VOC sensor	14
5.2	Nanocomposite sensors based on polymer/carbon nanotubes	14
5.3	Influence of atmospheric plasma on the sensor	14
5.4	Nanocomposite sensors based on graphene	14
6.	AIM OF THE DOCTORAL THESIS	15
7.	EXPERIMENTAL SECTION	16
7.1	Materials and chemicals	16
7.2	Preparation of substrates for percolation curve investigations	16
7.3	Electrical percolation: preparation of samples and measurement.....	16
7.4	Patterning of substrates for sensors	17
7.5	Preparation of (nano)composite layer	17
7.6	Procedure for the VOCs detection	18
8.	RESULTS AND DISCUSSIONS.....	19
8.1	Initial heuristics	19
8.1.1	Filler screening	19
8.1.2	Thermoplastic matrices and MWCNTs nanocomposites.....	19

8.1.3	Elastomer matrices and MWCNTs nanocomposites	19
8.1.4	Chemiresistive sensors MWCNTs with elastomeric matrices ...	20
8.2	Practical application of MWCNTs/elastomer sensors.....	24
8.2.1	Evaluation device for organic vapours	24
8.2.2	Microstrip antenna	25
8.3	Graphene nanocomposite.....	25
8.3.1	Why graphene	25
8.3.2	GNPs/SIS nanocomposite.....	25
8.4	Investigations of atmospheric pressure plasma jet (APPJ) modification 26	
8.5	Improvements in the sensing layer casting method.....	26
8.5.1	Automatic dip coating process.....	26
8.5.2	Spin coating process	26
8.6	Giant response and selectivity of SBS/GNPs room temperature sensor to organic vapours	27
8.6.1	Initial reconsiderations.....	27
8.6.2	Advanced experimental methodology	28
8.6.3	Electrical properties of SBS/GNPs nanocomposite films	29
8.6.4	Response and selectivity of the sensor	30
8.6.5	Sensing mechanism.....	32
9.	CONCLUSIONS	37
10.	CONTRIBUTION TO SCIENCE AND PRAXIS.....	39
	REFERENCES.....	41
	LIST OF TABLES	44
	LIST OF FIGURES	45
	LIST OF SYMBOLS AND ACRONYMS.....	46
	CURRICULUM VITAE	47

1. INTRODUCTION

1.1 Nanotechnology

Nanotechnology is a science, engineering, and technology and was first introduced in 1974 by Norio Taniguchi and defined as “processing of separation, consolidation of materials by one atom/molecule”. As a consequence, this term could be called the “processing of materials conducted in nanoscale, one billionth of a meter (10^{-9} m) in size [1]. Nanoscale materials are utilized for the application of extremely small things across many fields. Accordingly, carbon allotropes, especially carbon nanotubes, is nanotechnology useful for polymer composites, electromagnetic shielding, electron field emitters, capacitors, batteries, and structural composites [1, 2].

1.2 Polymer nanomaterials

For many years, we have known that better materials are composites such as filled polymers, where polymer fillers have a length scale in micrometres, and their interface of fillers is close to the bulk polymer matrix. The use of inorganic fillers in industry to modify polymers into products has experienced a revolutionary change from reducing the product/component cost to producing composites. As a consequence of the presence of nano-sized fillers, a large window of choices and opportunity is opened because nano-scaled fillers have a higher aspect ratio and fewer structure defects than their counterparts with micrometre-sized [2]. Polymer nanomaterials are classified into nanostructured materials with a wide range of nanometer size, from 1 nm to as large as 100 to 200 nm. Introducing nanoparticles as additives/fillers into polymer systems has claimed in polymer nanocomposites (PNs) like high-performance products. Based on these previous experiences, PNs are excellent modern materials where the length scale of nanoparticles is in nanometers. Nanostructured materials have a shorter distance between the polymer and the filler (nanofiller) and have a large representation per volume in the given polymer.

Research and development of nanomaterials provide us with unique opportunities to develop many revolutionary materials. For instance, the interaction between CNTs and polymer matrix has a limited enhancement. For electrical properties, a high amount of CNTs are added to a polymer, but the improvement of these electrical properties in composites is still limited due to random distribution and poor dispersion of CNTs. Their sizes, interparticle interactions, surface, purity, and resistivity determine many exceptional properties and performance. They are very attractive and have a great deal of attention because of their potential use in areas such as electronics, optics, healthcare, magnetic data storage, chemical industry, etc. These materials can be widely used for chemical and biological sensors, cell electrodes, and super-capacitors [3].

2. POLYMERS

Polymers form the main part of the composite material, which is imagined as the domain role in this work. Several polymers were tested, such as thermoplastic materials like styrene or acrylate polymers, but the results have shown no suitability for this purpose. Otherwise, due to their chemical impropriety, polyolefin materials were not a good candidate for experiments. Elastomers, with their elastic properties, seemed better choices for direct contact with organic vapours. Elastomeric matrices were the right way as an important part of future polymer nanocomposite. Thus, elastomeric polymers such as thermoplastic polyurethane, styrene-isoprene-styrene copolymer, and ethylene-octene copolymer appeared to be proven.

2.1 Styrene-isoprene-styrene copolymer (SIS)

The first and most used polymer for the preparation of the polymer composite was SIS – Kraton D 1165 PT. SIS is produced by ionic copolymerization, gradually introducing styrene, 2-methyl-1,3-butadiene (isoprene), and styrene in one reactor. Styrene content varies typically between 15 – 40 percent. The styrene has a function of domains of crosslinks, which provide mechanical properties like strength, hardness, and abrasion resistance, while the isoprene, the rubber matrix, provides flexibility, toughness, and abrasion resistance. SIS, with a low styrene content, has similar mechanical properties to those of vulcanized rubber. However, SIS elastomers can be processed with techniques used for thermoplastic polymers [4].

SIS has a unique molecular structure and properties compared to other plastics or rubbers. Each block has its own glass transition temperature, where the styrene block has $T_g = 95\text{ }^\circ\text{C}$ and the isoprene block has $T_g = -60\text{ }^\circ\text{C}$. This double-phase structure also gives “Kraton” high elasticity, low viscosity, easy thermoplastic processing, and dissolving in organic solvents. The rubbery isoprene blocks make this copolymer soft, with low viscosity and cohesiveness. On the contrary, styrene blocks provide high strength, hardness, and rigidity. Exposure to temperatures above $100\text{ }^\circ\text{C}$ is SIS transfer to melt the polymer and can be processed by plastic technologies such as extrusion or moulding. SIS block copolymers are blended with tackifier resins, oils, and fillers in many cases.

2.2 Thermoplastic polyurethane (TPU)

Polyurethane (PU) is a polymer that belongs to the group of amorphous thermoplastics, specifically polyesteramides. The beginning of history of polyurethanes dates back to 1937, when the research was conducted in Germany under the leadership of Dr. Otto Bayer, and after that, in 1941, linear polyurethane was developed for serial production.

The second polymer used to prepare the polymer composite was TPU – Desmopan 385 S. Its linear polymer chain consists of alternating flexible, elastic segments with a low T_g, and rigid, crystalline segments with a high melting point. It is therefore a modification of these segments that create unique properties, such as strength, hardness, stiffness, flexibility, always depending on the required applications. It also has high wear resistance, flexibility over a wide range of temperatures, high elasticity, excellent resistance to oils, greases and solvents, resistance to weathering and high-energy radiation [10, 11, 12].

2.3 Ethylene-octene-copolymer (EOC)

EOC copolymer consists of polyethylene (PE) and 45% octene, where octene has a major effect on the improved properties of this copolymer. The presence of octene causes a lower degree of crystallinity and higher flexibility of the copolymer. It has a very low density and not very good mechanical properties. It also has excellent "slip" and flow properties during processing. It is mostly used by injection moulding technology for automotive exterior or interior parts. EOC exhibits easy handling and mixing and is well soluble in toluene. In some applications, it is used as a substitute for ethylene-propylene rubbers [8].

The third polymer for the preparation of the polymer composite was EOC – ENGAGE 8842 Polyolefin elastomer. „Engage“ is the most used in automotive industry, for example in airbag systems, body panels, bumpers, exterior trims panels and the other industrial or consumer durable goods. It is also recyclable for in-process scrap re-use. It can be processed using extrusion, compounding, and thermoforming, too. Suitable for making tough and resilient yet flexible products [9, 10].

2.4 Styrene-butadiene-styrene co-polymer (SBS)

SBS is accessible thermoplastic elastomer which is produced by ionic copolymerization of styrene and butadiene. It has high tensile strength but is vulnerable to thermal and oxidative degradation. This type of SBS was 30 wt. % of styrene content.

Styrenic block copolymers are often used to enhance the performance of many products. They are widely used as direct moulded or extruded auto parts, sporting goods, and films, and also in sealants, gasket materials, hotmelt adhesives, rubber bands, toy products, shoe soles and others [11, 12].

For this research, it was selected as an alternative polymer for SIS due to its similarity in properties, styrene content and description and due to its availability as a standard chemical.

3. CARBON ALLOTROPES

Carbon and its miscellaneous forms have been in technology since prehistoric times. Charcoal, graphite, and carbon black have been used as writing, drawing, and printing materials. Charcoal has been used as fuel and played an important role in humankind's first technology. In 1896, Edward Acheson, an American, made the first synthetic graphite. In the twentieth century, the relevance of activated carbon provided engineers with the 1950s invention of carbon fibres - a new lightweight and ultrastrong material. The development of synthetic methods opened the way for industrial use, and carbon science was widely broadened [13]. Carbon has many forms that exist with nanoscale dimensions. This material occurs in multiple forms with different atomic structures [14]. Carbon nanotubes, graphene, and superconductive carbon black are used for this research.

3.1 Carbon nanotubes

Carbon nanotubes (CNTs) are a form of carbon and represent structured carbon atoms that look like beehives. CNTs are one of the modern forms of carbon. Their unusually tubular shape with hexagon-structured carbon atoms is one of the most promising materials for current research in polymer electronics. In 1991, carbon nanotubes were discovered by a Japanese researcher, Sumia Iimijima, who described their composition [15]. Carbon nanotubes have high mechanical strength, stiffness, high specific surface, and unique electrical conductivity. These properties are interesting in developing new composite materials, sensors, electronic devices, separation membranes or filters, microstrip antennas, smart shoes, and other wireless devices.

The nanotubes can be produced either in the single-wall form or in the form of multiwall carbon nanotubes (MWCNTs). The production of MWCNTs is relatively simple, and they are available in a large variety of commercial brands. Moreover, they have a large specific surface area and good electrical conductivity [16].

3.2 Graphene

The history of graphene began in 1947 during a theoretical study of the electrical behaviour of graphite by physicist P. R. Wallace. In 2004, it was discovered with a mechanical exfoliation method called "scotch-tape" by researchers A. Geim and K. Novoselovm, where the layers from graphite are removed with used adhesive tape. Graphene is described as a two-dimensional (2D) graphite sheet and can be described as self-assembled vertical sheet nanostructures called graphene nanowalls (GNWs). Graphene is electrically conducting, strong, and flexible, and it is a very promising material for many applications, such as transistors (up to a frequency of 1 THz), microprocessors, and memories [17].

4. COMPOSITE / NANOCOMPOSITE

A composite is a material which is made from two or more different materials with significantly distinct properties. Composites are symbolized heterogeneous systems made with a combination of materials to form an overall structure. They are produced in multiphases with different mechanical and physical properties. The main phase is the polymer matrix and the second phase is a filler. The resulting composite should be homogeneous and have the same properties in all parts, i.e., be synergetic. The filler/reinforcement has better properties than its own polymer matrix [18].

A filler usually represents particles in various forms (spheres, plates, fibres). When the size of the particle is 10^{-8} m and bigger, it is a composite. Another innovative group are nanocomposites, where the filler particle size is 10^{-9} m. Nanocomposites have one from their phases in nanometers or structure have in nano-scale [18].

4.1 Electrical percolation threshold

The percolation theory determines the conductivity of composite/nanocomposite materials. The main factor is the concentration of electrical conductivity filler. A process of charge transfer is between two particles, and the distance between them is important. In low concentrations, conductive particles are separated by a non-conductive polymer matrix, and charge transfer occurs using the principle of hopping or tunnelling. The principle of hopping or tunnelling can occur if the particle distance is less than 10 nm. If the distance is greater, the process cannot occur, and the conductivity of the self-polymer matrix gives the conductivity. Increasing particle distance decreases the transfer of electric charge between the two conductive filler particles.

The most fundamental term is the percolation threshold. It is a minimum concentration of conductive filler or point where a conductive chain of macroscopic length is created. If the concentration is increased in the polymer matrix, it leads to building a macroscopic network of conduct paths (percolation area), and electrical conductivity increases [19].

Polymer composite materials show electrical conductivity due to their conductive fillers, where the nanoparticles are closely bound to each other and contained in the entire volume of the matrix. The low filling content of the conductive particles shows a low conductivity of the composite. Large amounts of filler particles cause lower values of electrical resistance. The electrical conductivity of composites is sensitive to the number of conductive pathways and occurs in highly filled matrices or matrices with an uneven distribution of nanofillers [20].

4.2 Advantages of nanocomposites

In view of nanotubes or other carbon allotropes, their possession of electrical conductivities is subject to many researchers. CNTs can impart electrical conductivity to polymers with a minimum amount of CNTs (with a continuous network of CNTs) or a minimum percolation threshold. Very important for this parameter are factors: CNTs type (SWCNTs or MWCNTs), its aspect ratio, synthesis technique, degree of dispersion, alignment, and essentially polymer matrix.

Percolation thresholds have been found to be much lower than other fillers like metal particles or carbon black. A recent review concluded that the type of polymer and dispersion method play the biggest role in defining the minimum percolation threshold than the type of CNTs [21].

4.3 Preparation of carbon nanotube/polymer composites

In scientific literature, three types of preparation CNTs/polymer composites are mentioned. The first one, the simplest method, is solution mixing. It involves mixing nanotube dispersions with solutions of the stated polymer and then evaporating the solvents in this controlled way. Solution mixing has been used with a range of polymers; the nanotubes are often functionalized prior to adding to the polymer solution. Sometimes can be a problem with the compatibility of functional groups with the polymer matrix, but to avoid this, the nanotubes can be functionalized with polymers that are structurally similar to matrix polymers. Another procedural method is using a high-energy ultrasonic probe to disperse the current carbon filler (e.g., MWCNTs in toluene) and then mixing the dispersed suspension with a dilute solution of polymer (e.g., styrene-isoprene-styrene or other elastomeric or thermoplastic polymers) and again with ultrasonic agitation [22].

5. SENSOR

A sensor is a device that detects and responds to electrical or optical signals. These electrical quantities can ensure good sensitivity, focus, and signal transmission accuracy. Sensors are widely used because they are able to show detection and scanned data precisely.

The essence of the sensor's function is in measuring external stimulus and its behaviour or reaction. It means scanning of measuring physical, chemical, or biochemical values (reactions) and consequent transport of the information about results from measuring. The main parts include a data scanner, signal converter, and evaluation system. Sensors can be produced in tiny dimensions, and they have a high accuracy in measuring, sensitivity, secure transfer of signal, low noise real-time analysis, etc. [23, 24].

5.1 VOC sensor

Volatile organic compounds (VOCs) are organic chemicals that are contained in the gases from solids or liquids. They include many chemicals or compounds emitted from a wide range of man-made or naturally occurring products.

Sources of VOCs can be found in many areas, like indoor or outdoor, and in products such as solvents, paints, aerosols, stored fuels, adhesives, cleaners, and many others. Concentrations of many VOCs are usually higher indoors (up to ten times higher) than outdoors. Sensors are designed for monitoring common air quality contaminants. The VOCs sensors can be used to directly measure ambient concentrations of a broad range directly[24].

5.2 Nanocomposite sensors based on polymer/carbon nanotubes

Many of the outstanding properties of carbon nanotubes, graphene, and carbon black were outlined. For the preparation of polymer composites with some conductive fillers (e.g., CNTs), a method by mixing nanotube dispersion with solutions of the polymer and then evaporating the given solvent is used. A composite material base on polymer/CNTs has a largely very good electrical and thermal conductivity. These types of sensors are mostly utilized as pressure sensors or motion sensors that record changes of deformation in real-time or as sensors for detecting volatile organic compounds, which work essentially on changes of electrical resistance during absorption or desorption of these organic solvents [25].

5.3 Influence of atmospheric plasma on the sensor

Plasma treatment can be considered as a technique for surface functional modifications. Atmospheric plasma can help for systematic studies on the effect of the plasma excitation method on the polymerization or practical impact of its effect on the polymer's layer surface [26, 27].

5.4 Nanocomposite sensors based on graphene

Graphene attracts most of the attention in contemporary literature due to its nanoscale dimensions and conductivity applicable across many fields. Since the discovery of graphene and its two-dimensional single-layer honeycomb arrangement of sp^2 hybridised carbon atoms structure by A. Geim and K. Novoselov in 2004 [28] the number of publications has grown explosively. Nowadays, there are more than 300,000 papers listed in the Web of Science database. The interest in graphene seems to find its saturation point in a number of ca 40,000 publications per year in the last four years [29].

6. AIM OF THE DOCTORAL THESIS

The broader scope of the thesis is to prepare novel enhanced sensors based on polymer matrix nanocomposites with carbonaceous fillers. Although numerous applications in sensors for volatile organic compounds (VOCs) have been reported for these materials, they still mainly suffer from low selectivity and low sensitivity. The general sensing mechanism is based on the interaction of adsorbed analyte molecules (VOCs) with the nanocomposite, resulting in a change in the quality of the contacts (charge transfer) between the individual filler particles, which is macroscopically manifested as a change of the sensor's resistance.

The aim of the thesis is to prepare chemiresistive sensors with enhanced sensitivity and selectivity to selected VOCs based on thermoplastic elastomer copolymer matrix nanocomposites with multiwall carbon nanotubes (MWCNTs) and graphene nanoplatelets (GNPs) used as conductive fillers. Unlike in previous works devoted to modification and functionalization of the filler particles, here, the role of the polymer matrix is investigated, as it may also impart sensitivity and selectivity to the sensor.

Therefore, the following goals and objectives had to be accomplished, including the trial and error method, to attain the aim of the thesis.

1. Initial heuristic
 - a. Preliminary screening of the fillers, testing of carbon black, carbon fibres, MWCNTs as possible candidates, and selection of the most promising filler.
 - b. Preliminary screening of thermoplastic (polystyrene, PS, and polymethylmethacrylate, PMMA) and thermoplastic elastomer (thermoplastic polyurethane, TPU, ethylene-octene copolymer, EOC, styrene-isoprene-styrene copolymer, SIS) polymer matrices for their suitability to be used in the proposed kind of sensors and selection of best candidates.
2. Preparation and study of sensors based on nanocomposite films combining the best filler candidate with selected polymer matrices. Comparison with *state-of-the-art* buckypaper sensor.
3. Exploration of further enhancements of the sensors:
 - a. Introduction of graphene filler.
 - b. Physical modification of the sensor's nanocomposite layer by cold plasma.
 - c. Variation of preparation method: manual and automatic dip coating, spin coating, alternation of SIS for styrene-butadiene-styrene (SBS) matrix.
4. Graphene filler SBS co-polymer nanocomposite-based sensor: preparation and study of its response and selectivity mechanism.

Note: Points 3 and 4 were clarified after the completion of the first stage of the research.

7. EXPERIMENTAL SECTION

The experimental part of this thesis describes the creation of gas sensor samples for the detection of VOCs in the air. Two classes of sensors were examined, the first class is based on MWCNTs and the other class is based on GNPs. The characterization methods used throughout the work are also described, mainly the testing of sensor properties.

7.1 Materials and chemicals

Polymers make up the main part of composite materials, which are the core of this thesis. In the past were tested more polymers, thermoplastic polymers like polystyrene and polymethylmethacrylate, but as proven polymers were predominantly elastomeric polymers like styrene-isoprene-styrene, thermoplastic polyurethane, and ethylene-octene copolymer.

MWCNTs were fabricated with CVD method from acetylene precursor and were supplied by Sun Nanotech Co. Ltd., China. The diameter of the nanotubes used is 10 - 30 nm, length 1 - 10 μm , purity > 90 % and specific electrical resistance 0.12 $\text{S}\cdot\text{cm}^{-1}$. Graphene, precisely Graphene nanoplatelets xGnP M-5, are unique nanoparticles consisting of short stacks of graphene sheets having a platelet shape and were purchased in Sigma Aldrich. Particles have an average thickness of approximately 6-8 nm and a typical surface area of 120 to 150 m^2/g , density 0.03-0.1 g/cm^3 , product number 900412.

Toluene is one of the tested VOCs. It is a solvent and was used to form a polymer solution of SIS and EOC. It also served for its own measurement when it was detected by prepared sensors. Ethanol, acetone, and heptane were tested as well.

7.2 Preparation of substrates for percolation curve investigations

Electrodes for measuring the percolation curve were prepared from Cuprexit FR-4. It is the layered structure which is made of 1 mm thick epoxy/glass laminate coated with a 35 μm thick Cu foil (Bungard Elektronik GmbH & Co. KG, Windeck, Germany) by using a 30% solution of FeCl_3 (Sigma-Aldrich Inc., St. Louis, MO, USA) in water at room temperature. Subsequently, the rectangular electrodes (sized 50 x 20 mm) were dipped into each polymer dispersion. The ensuing films were about 150 μm thick.

7.3 Electrical percolation: preparation of samples and measurement

Determination of the weight fraction for the polymer solution:

$$w = \frac{m p.}{m p.+m s.} * 100 (\%) \quad (1)$$

where, w is the weight fraction (%), $m p.$ is the polymer weight (g), $m s.$ is the solvent weight (g)

$m s.$ is determined as:

$$\rho = \frac{m s.}{V} \Rightarrow m s. = \rho * V \quad (2)$$

where, ρ is the density of organic solvent (g/cm³), V is the volume of organic solvent (ml)

Materials used for preparation: SIS in toluene: $\rho = 0,867$ g/cm³, TPU in dimethylformamide: $\rho = 0,944$ g/cm³, EOC in toluene: $\rho = 0,867$ g/cm³

The amount of carbon fillers (to the amount of polymers) was then calculated to each concentration:

$$w = \frac{x}{x+m p.} (g) \quad (3)$$

where, w is the mass fraction of carbon filler concentration (%), $m p.$ is polymer weight (g), x is the calculated amount of carbon filler (g)

The electrical conductivity was estimated from resistance measurements performed by utilising Keithley 6517B, (Tektronix, Inc., Beaverton, OR, USA) instrument to obtain the percolation curve of the sample. Each sample was connected with the use of the two-point method.

7.4 Patterning of substrates for sensors

Interdigitated electrodes (IDEs) are one of the most popular transducers. They are widely utilized in technological applications, especially in chemical sensor, due to their inexpensive manufacturing, ease of fabrication process, and sensitivity. For the purpose of detection and analysis, the electrodes are able to obtain a signal for practical measuring. The electrodes are usually fabricated in small sizes. The electrode used for self-measurement is also made of Cuprexit material. The gaps between the individual "ridges" on the electrode are at a distance of 0.5 mm. The electrode for the self-measurement was chosen because it has a large number of contact points, which are very well suited for the preparation of electrodes for the detection of organic vapours. The electrode is light, has small dimensions, its production is cheap, and the evaluation of results is fast and efficient.

7.5 Preparation of (nano)composite layer

A polymer solution (in toluene) was prepared for the production of samples for (nano)composite preparation. Prepared films were used for percolation measurements and for the initial assessment of the sensors' performance in the preliminary screenings. Initially, manual dipping was used for casting the

nanocomposite films, then automatic dipping was tested, and finally, spincoating was applied as the best method. The advanced methods and experiences gathered in their further development are described in the respective parts of the results and discussion of the Thesis.

7.6 Procedure for the VOCs detection

This work aims to create a polymer composite that serves as a sensing unit for the detection of selected VOCs. The electrode has a layer of polymer composite with a conductive function. The electrical resistance was measured using a Multiplexed Data Logger 34980A (Keysight Technologies, Canada) connected to a PC, where the measured resistivity data was read every 1 s. The electrode with the active scanning layer was closed in an Erlenmeyer flask containing an organic solvent. These organic vapours were either an aliphatic hydrocarbon (heptane), aromatic hydrocarbon (toluene), ketone (acetone) or alcohol (ethanol). It took 6 min before the electrode with an active layer detected organic solvent vapours by changing its electrical resistance. The nanocomposite electrical resistance was quantified by the relative electrical resistance change defined as:

$$\Delta R/R_0 = \frac{(R - R_0)}{R_0} \quad (4)$$

where: R_0 is the stabilised electrical resistance of the composite before the exposition to vapour (Ω) and R is the resistance during the exposition of the holder with the coated interdigitated electrode by the nanocomposite (Ω)

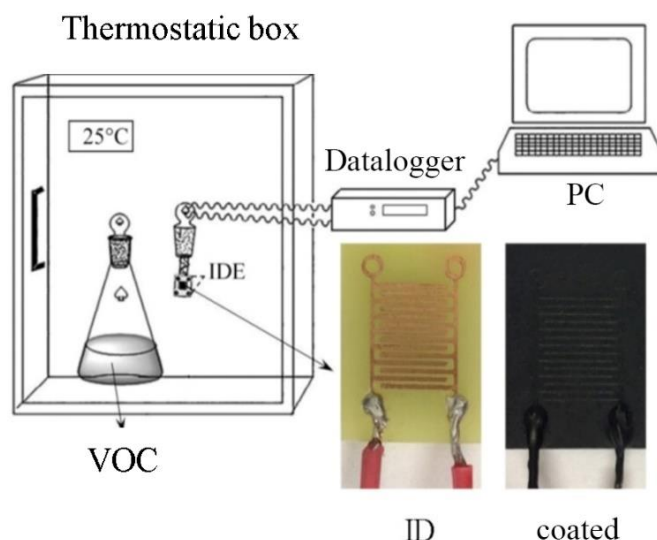


Figure 1: Experimental system for measuring resistance change [RS1]

After this time, the electrode was pulled out of the flask, and the desorption cycle was started in the thermostatic box for 6 minutes at 25 °C. These cycles of absorption/desorption were repeated five times. The measurement was made under atmospheric pressure, at a temperature of 25 °C and relative humidity of 40 % in the thermostatic box.

8. RESULTS AND DISCUSSIONS

8.1 Initial heuristics

8.1.1 Filler screening

The first task was to choose the right filler for the polymer matrix. Firstly, three types of carbon-based fillers, namely Multiwall Carbon Nanotubes (MWCNTs), Carbon Fibers (CF) and Carbon Black (CB), were selected and tested. Graphene nanoplatelets (GNPs) were added to the experimental design later.

8.1.2 Thermoplastic matrices and MWCNTs nanocomposites

Brittle thermoplastic matrices have been chosen for volatile organic compound detection due to comparison with elastomeric matrices. Specifically, polystyrene (PS) and polymethylmethacrylate (PMMA) were tried for this purpose.

Polymer composites consisted of PS and PMMA with 11 % of MWCNTs, which were tested for acetone vapours during 2 cycles of adsorption/desorption, a total of 24 minutes (1440 seconds). Resistance was recorded to identify any response. These tests demonstrate that PS and PMMA thermoplastic matrices are likely not suitable for sensor application, at least in the intended way.

8.1.3 Elastomer matrices and MWCNTs nanocomposites

Three thermoplastic matrices were initially examined for their suitability for the fabrication of chemiresistive VOCs sensors.

All these three materials exhibit easy handling and mixing and are well soluble in toluene. The composites were prepared by dispersing the corresponding amount of the filler in the copolymer solution in toluene and manually dip-coating the pre-patterned substrate, as described in experimental part. All tested filler concentrations are summarised in Table 1 A). According to the method described in the experimental part, the resistivity of each composite sample was evaluated. Collected data are plotted in the Graph in Figure 2. The shape of percolation curves is not very well developed. Nevertheless, the concentrations corresponding to the resistivity ca 300 Ωcm were selected as suitable for the fabrication of the sensors' samples. The resistance of any tested sensor specimen must be measurable and small enough to provide range for the resistance increase when the sensor is exposed to the saturated VOCs. These concentrations are indicated in Table 1 B).

Table 1: Compositions of tested samples for percolation threshold estimation A) for MWCNTs. Part B) shows the selected compositions for the preparation of testing Sensor specimens

A)		B)	
Polymer	Content of MWCNTs (%)	Polymer	Content of MWCNTs (%)
SIS	2, 5, 8, 11, 14, 17	SIS	11
TPU	8, 11, 14, 17, 20, 21, 23	TPU	23
EOC	21, 24, 27, 30, 33, 36	EOC	36

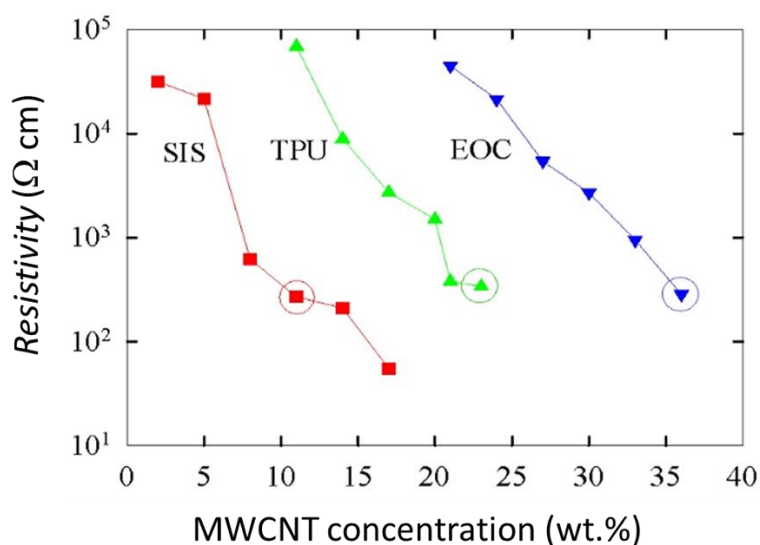


Figure 2: Percolation curve - Dependence of the electrical resistivity of MWCNT/copolymer composites on nanotube concentrations. The circles denote the given composites, which had nearly identical resistivity of 300 Ωcm and hence were subsequently used for the comparison of the vapour effects.

8.1.4 Chemiresistive sensors MWCNTs with elastomeric matrices

Three nanocomposite materials with comparable resistivity were prepared from elastomeric copolymers with MWCNTs filler. Styrene-isoprene-styrene (SIS), thermoplastic polyurethane (TPU) and ethylene-octene copolymer (EOC) were the elastomeric matrices. The nanocomposite films were used as transducers in the sensors to detect ambient organic vapours of different polarities such as ethanol, acetone, toluene, and heptane. Adsorption and desorption cycles were measured in a 6-minute period. One measuring cycle was 12 minutes. The whole measurement took place in 5 cycles, 60 minutes overall.

The responses of the sensors to each of the tested vapours are plotted in Figures 3, 4, 5. The sensor response to the on/off cycle was recorded for five cycles. The curves have a typical shape of adsorption/desorption response. The adsorption of vapour molecules causes an increase in the electrical resistance, while desorption of vapour molecules results in its decrease.

The different sensitivity of the sensor towards the tested chemicals is manifested in each response record in the figure below. The presence of ethanol vapours produces only little change in the resistance. Acetone vapours have a small yet pronounced impact on the resistance change. By far, the highest sensitivity was observed for heptane. In other words, the selectivity of the sensor was clearly confirmed by this experiment.

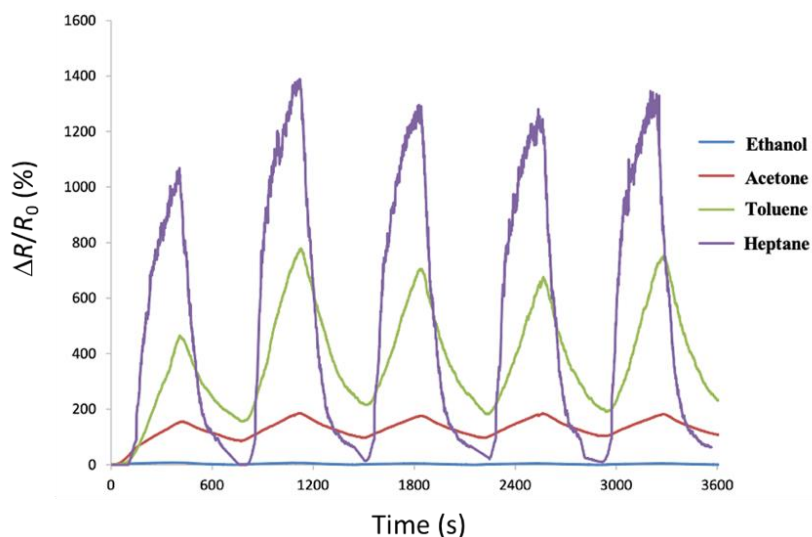


Figure 3: Graph of the sensitivity of the SIS/MWCNTs sensor during the absorption/desorption cyclic phase for vapours of all solvents [RS1]

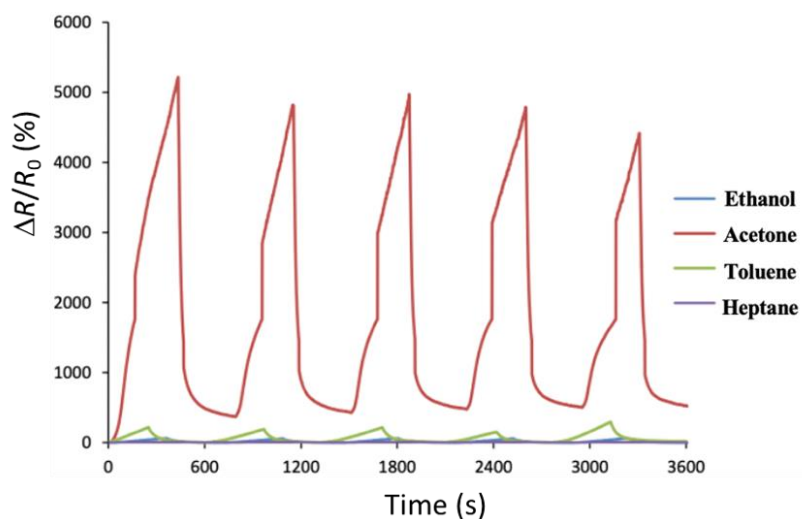


Figure 4: Graph of the sensitivity of the TPU/MWCNTs sensor during the absorption/desorption cyclic phase for vapours of all solvents [RS1]

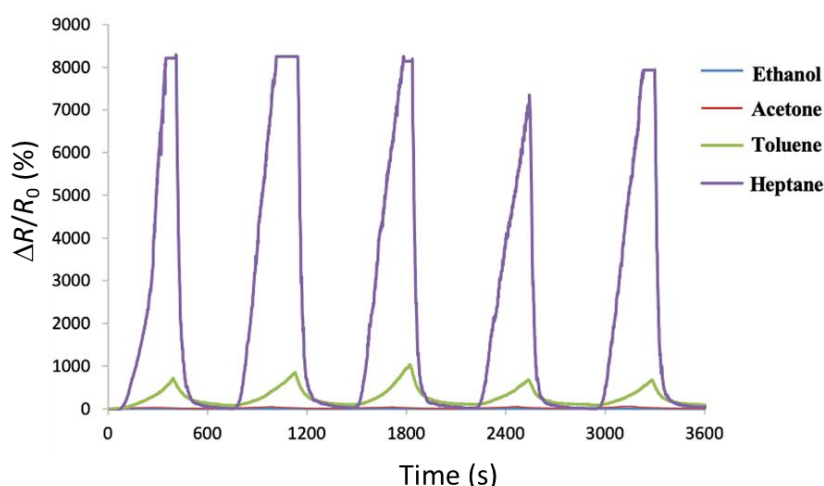


Figure 5: Graph of the sensitivity of the EOC/MWCNTs sensor during the absorption/desorption cyclic phase for vapours of all solvents [RS1]

Table 2 summarizes the maximum values $\Delta R/R_0$ for each composite sensor with the specific content of filler and for each solvent. The response of the sensor correlates with the hydrophobicity of the vapour molecules. Especially for SIS/MWCNTs sensor, ethanol is a polar compound that neither swells nor permeates the hydrophobic copolymer matrix. According to its molecular structure, acetone is slightly less polar than ethanol and is expected to permeate the copolymer matrix slowly, which results in the observed relatively small sensitivity among tested compounds. Toluene has a moderate influence on the resistance change, which is in accordance with its ability to dissolve both the styrene and isoprene blocks of the copolymer and moderate permeability through the copolymer. The highest sensitivity of the sensor was observed for heptane. It correlates with the structure of heptane, which is of aliphatic hydrocarbon character that can be considered similar to the molecular structure of the major polyisoprene block component of the elastomer.

Table 2: Results of max. values $\Delta R/R_0$ of composite materials (sensors) in a given solvents [RS1]

	SIS	TPU	EOC
Solvents	$\Delta R/R_0$ max. (%)	$\Delta R/R_0$ max. (%)	$\Delta R/R_0$ max. (%)
Ethanol	8	62	2
Acetone	181	5198	56
Toluene	761	291	1025
Heptane	1388	11	8287

The observed changes most likely resulted from the penetration of the vapour molecules into the polymer matrix, which subsequently swelled and increased the distances between the carbon nanotubes. As a result, the charge transfer between

conductive filler particles was impeded, and the percolating conducting paths were disrupted, which is manifested as a significant increase in the measured resistance of the sensor. The most remarkable change in gas sensor electrical resistance (over 8200 %) was made from the carbon nanotube/ethylene-octene copolymer and was elicited by the non-polar heptane.

Obtained results can be compared with a recent reference, a sensor based on the matrix-less material, called buckypaper, prepared from pristine, yet modified, bare MWCNTs via a vacuum filtration technique, which is reported elsewhere <https://doi.org/10.1016/j.mee.2020.111403>. The buckypaper sensor was exposed to the saturated vapours of the same set of VOCs under the same conditions, and the data are summarized and illustrated in Figure 6. It is clearly visible that the buckypaper based sensor provides the lowest selectivity among the tested sensors. Moreover, the polymer matrix sensors provide higher relative responses in general. These observations make the proposed sensors good candidates for further research and give the promise to overcome the MWCNTs solely based sensor. [RS2]

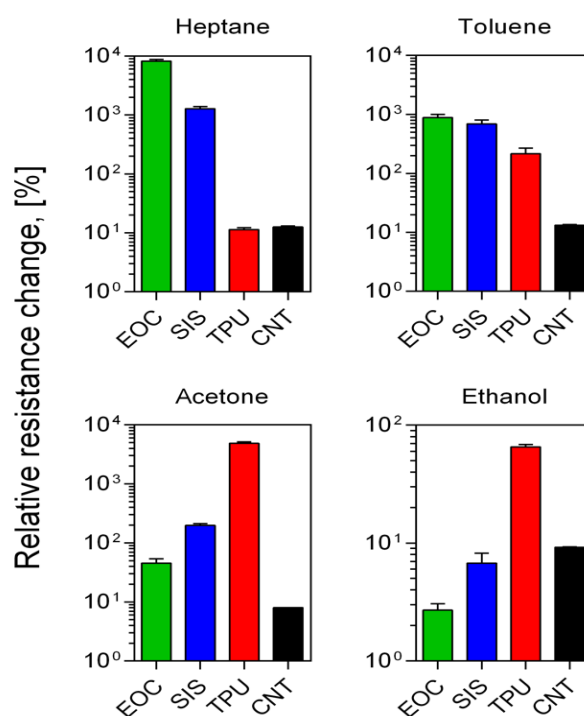


Figure 6: Maximal relative resistance changes (sensitivity) of the given MWCNTs/copolymer composite sensors and a pristine MWCNT network (buckypaper) upon exposure to the indicated chemical vapours. Composites are denoted in the figure as TPU, SIS and EOC, and pristine MWCNT networks as CNT. Data are depicted as means \pm SDs ($n = 5$). [RS2]

8.2 Practical application of MWCNTs/elastomer sensors

8.2.1 Evaluation device for organic vapours

The preliminary results indicated that these composites are suitable materials for easy manufacturing of inexpensive deformable vapour sensors, which can be readily adjusted to limited space or an unconventional shape.

The evaluation device for organic vapours serves to identify samples of organic compounds based on measurement changes of electrical resistance from two particular devices fabricated from carbon nanotubes in different polymer matrices SIS and TPU, which provided the best resolution between polar and non-polar VOCs. This evaluation device recognizes the type of organic solvent based on results of previous measurements characterizing differences in the two types of particular sensors.

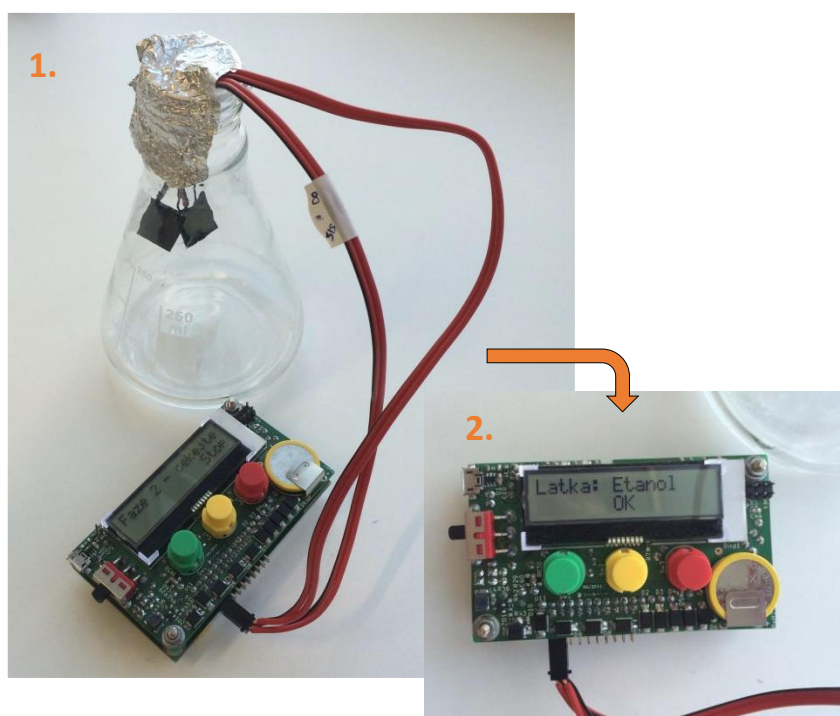


Figure 7: Device for evaluation of organic vapors, a primitive “electronic nose”. The upper image shows the device in the off-state, two particular sensors are visible. The lower pair of images show actual measurement 1) during self-evaluation, 2) display of the evaluated solvent [RS1]

The results demonstrated that the sensors using developed composites are able to detect ambient organic vapours, which selectively alter their electrical resistance. In this simplest construction, the choice of polymer matrix imparts the selectivity to the sensor and thus allows resolution between saturated vapours individual VOCs within the tested set of the four selected VOCs (ethanol, acetone, toluene and heptane). Moreover, the gas sensor demonstration prototype developed in our research is small in size and production costs are low. It shows the way to devices that could be practically used as a part of a universal device for the identification of organic solvent vapours, the so-called "electronic nose".

8.2.2 Microstrip antenna

Another demonstration of the practical application of the developed nanocomposite sensing material is the fabrication of a microstrip antenna with sensing properties.

A wireless microstrip antenna-based sensor samples were made from MWCNT nanocomposite using the three matrices TPU, SIS and EOC. The biggest sensing responses of the microstrip antenna-based sensor were observed for the sample made from MWCNT/EOC nanocomposite exposed to heptane saturated vapours. Thus, this composition was selected for further studies. [RS2]

8.3 Graphene nanocomposite

8.3.1 Why graphene

With respect to the first and second goals, the effect of proper polymer matrix and MWCNT filler choice on the sensitivity and selectivity of the sensors has already been demonstrated. The materials performed better in comparison with the buckypaper reference. Nevertheless, the work continued to attain even better results, something that could fulfil the promises of nanotechnology. Therefore, the research focused on the preparation of sensors with graphene filler.

8.3.2 GNPs/SIS nanocomposite

Graphene is one of the miscellaneous forms of carbon. Carbon is exceptional in forming many allotropes due to its valency, which means structurally multiple forms of the same element with different atomic structures. Graphene has a large specific surface area and unique mechanical and electrical properties, especially electrical conductivity, which play an important role in this research due to its sensitivity to volatile organic compounds and gases. Namely, graphene is a perfect nanomaterial for measuring and sensing volatile organic compounds by a simple sensor made from copolymer composite, which is based on an elastomeric matrix and graphene as the electrically conductive filler. The polymer matrix imparts necessary selectivity to the sensors. Based on the previous results, SIS was selected as a suitable material. Thus, the graphene/SIS nanocomposite serves to these applications and make progress to the next steps. All tested filler concentrations are summarised in Table 3 A). According to the method described in the experimental part, the resistivity of each composite sample was evaluated. The resistance of any tested sensor specimen must be measurable and small enough to provide a range for the resistance increase when the sensor is exposed to the saturated VOCs. Therefore, the concentration indicated in Table 3 B) was selected.

Table 3: Compositions of tested samples for percolation threshold estimation A) for various concentrations of graphene. Part B) shows the selected compositions for the preparation of testing Sensor specimens

A)		B)	
Polymer	Content of Graphene (%)	Polymer	Content of Graphene (%)
SIS	1; 2.5; 3.75; 4.5; 5; 7.5; 10; 15; 20	SIS	7.5

8.4 Investigations of atmospheric pressure plasma jet (APPJ) modification

With the help of manual dip coating method, the nanocomposite layers were achieved. Another research activities were approach to knowledge to influence of nanosensor's surface by atmospheric plasma treatment. The proper filler concentration just above the percolation threshold is the primary key to the maximum sensitivity of the sensor. Additional secondary treatment of the surface of the sensor by atmospheric plasma can decrease the electrical resistance of the thin film and further improve the sensitivity of the sensor. Thus, the properties of the sensor may be tuned and further enhanced by atmospheric plasma.

8.5 Improvements in the sensing layer casting method

8.5.1 Automatic dip coating process

In my doctoral research, the dip coating was selected as a good candidate for the fabrication technique. The manual dipping operation looked easy, quick, and non-demanding, but it suffered from relatively poor reproducibility, repeatability, and homogeneity of the prepared film thicknesses. The acquisition of an automatic dipping machine led to efforts to improve this method.

Hence, this method was not successful for this purpose due to irregular layers on the whole surface of the electrode. The process was based on dipping in polymer solution **SIS/GNPs with 7,5 wt. %** of graphene in toluene. Regarding this operation, it is hard to obtain the film with the same reproductive thickness of the layer every time. It was tried to change the dipping time (less and more), distance for immersion (with also gradual immersion), and time for drying, but any change of procedure setting was not good for perfect performance and constant layer for our purpose - with either same or similar layer thickness. This method was selected as inappropriate for further research.

Based on this experience, the new motivation was to find a better method for our precise purpose of constant nanocomposite thin layers.

8.5.2 Spin coating process

As mentioned above, working with graphene was different from working with CNTs. Although this is an empirical fact based on my experience and the reasons

for this behaviour were not studied, it hypothesises that the 2D graphene has a much larger surface, resulting in larger surface energy and better geometrical features for reassembly than 1D CNTs in a thick solution of the polymer.

Spin coating is a procedure used to apply thin films on flat substrates or surfaces. It is one of the most widespread and simplest methods used to prepare polymer films. A polymer solution is applied to the centre of the substrate, obviously with a volume around several tenths of millilitres [30]. Reaching a symmetrical surface is accomplished by convection and diffusion in flowing gas. Spin coater secures control of the process and permits a better stable design of the product [31].

An average film thickness of 9.1 μm with a standard deviation of 0.9 μm was achieved for a representative series of five consecutively deposited layers. The standard deviation corresponds to the relative deviation of 10 %, implying the spin coating method as the best fabrication procedure among tested methods.

8.6 Giant response and selectivity of SBS/GNPs room temperature sensor to organic vapours

A chemiresistive VOC sensor with considerable sensitivity and selectivity was prepared using styrene-butadiene-styrene co-polymer (SBS) matrix filled with graphene nanoplatelets (GNPs) as the nanocomposite transducing layer deposited by spin coating on a copper interdigitated electrode (IDE) patterned substrate.

8.6.1 Initial reconsiderations

In contrast to the intriguing chemistry of the gas-sensing graphene-based elements described in the introductory chapter: Nanocomposite sensors based on graphene, the mechanism of strain sensors and their design is much simpler. First, selectivity is not an issue. Next, the response is based on the conductivity of graphene or any other conductive filler network, which is dispersed in a polymer matrix and whose conductivity depends on percolating pathways established by contacts of the filler particles. Hopping and tunnelling are the two possible mechanisms of charge transfer in and between otherwise electrically conductive filler particles separated by a thin enough layer of the insulating polymer matrix. The overall conductivity of such a network depends on the concentration and quality of contacts between single filler particles, particle aggregates and agglomerates. Then, the response of such strain sensors depends on changes in these conductive bridges induced due to the geometrical deformation of the network induced by the strain. In other words, the strain response of the graphene network mainly depends on the changes in the contact resistance of adjacent graphene sheets [32]. If the interparticle contact creates a narrow neck limiting the overall conductivity, the adsorption of gaseous molecules will influence the resistance response of such material as much as it changes the quality of these contacts. Our previous work on carbon nanotube entanglements demonstrated this sensing mechanism [33, 34]. [RS3]

8.6.2 Advanced experimental methodology

The preparation of the GNPs/SBS nanocomposite-based sensor required modification of the previous experimental procedures and integration of the best sensing film deposition method, i.e. spin coating. Following paragraphs restate the procedure for clarity and to present the advances in sample preparation method in a comprehensive way.

The electrical resistance response of the sensors is Sensitivity ($\Delta R/R_0$, [%]). The sensitivity was quantified as the relative electrical resistance change defined as:

$$\Delta R/R_0 = \frac{R - R_0}{R_0} \cdot 100 \% \quad (5)$$

The maximum sensitivity (R_{max}/R_0 , [%]) is the sensitivity of the sensor observed at the partial pressure of saturated vapour of a given VOC at 25 °C.

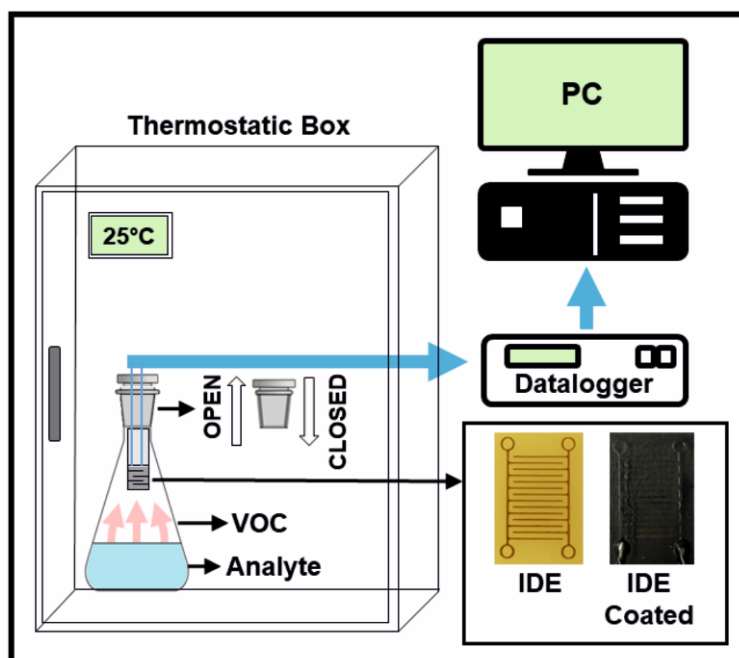


Figure 8: Experimental system for measuring the resistance change response to saturated vapours of tested VOCs [RS3]

The selectivity ($\sigma_{1/2}$) is defined as the mutual property of a pair of gasses (vapours) indexed by 1 and 2, comparing their maximum sensitivities normalised to corresponding to the partial pressure of their saturated vapours (p_0).

$$\sigma_{1/2} = \frac{R_{max,1}/R_0}{R_{max,2}/R_0} \cdot \frac{p_{0,2}}{p_{0,1}} \quad (6)$$

Cross sensitivity towards humidity was studied using mixtures of tested liquids with water. As toluene and heptane are immiscible with water, the vapours in the Erlenmeyer flask were composed of saturated vapours of the respective VOC and water. In the case of acetone and ethanol, mixtures of water with the respective VOC were used to generate the gas phase of equilibrium composition.

8.6.3 Electrical properties of SBS/GNPs nanocomposite films

The resistivity of SBS/GNPs films with various filler concentrations was investigated to find a suitable concentration for preparing the active layer in the proposed sensors. The percolation curve in Figure 9 displays the increase of electrical conductivity with increasing concentration of the filler. The electrical conductivity of the SBS/GNPs composite follows the percolation theory, stating that conductivity increases by many orders above a critical filler fraction, which is called the percolation threshold. Below this threshold, the material is insulating, whereas it behaves like a conductor above the threshold [35]. The concentration of the graphene nanofiller was varied as the factor determining the conductivity of the resulting material, whereas the fabrication method was kept the same for all samples. The mechanism governing the percolation behaviour of SBS/GNPs is expected to be similar to carbon nanotube-filled composites [36]. The conductivity of the SBS/GNPs is very low at mass percent values below 5 % due to the low amount of added GNPs. The biggest jump by eight orders in conductivity is between 4.5 % and 10 %, indicating the threshold at 5 % when large clusters begin to be formed and the tunnelling effect between GNPs is manifested. Connections between smaller clusters create a conductivity path at percolation. Further increase in GNPs concentration creates a network of filler particles. Above 10 %, the GNPs network is formed, and a further increase in concentration only densifies its structure, manifested in incremental conductivity enhancement. At high filler concentrations, the conductivity is stabilised by a high concentration of multiple connections between filler particle clusters penetrating the whole volume of the material. [RS3]

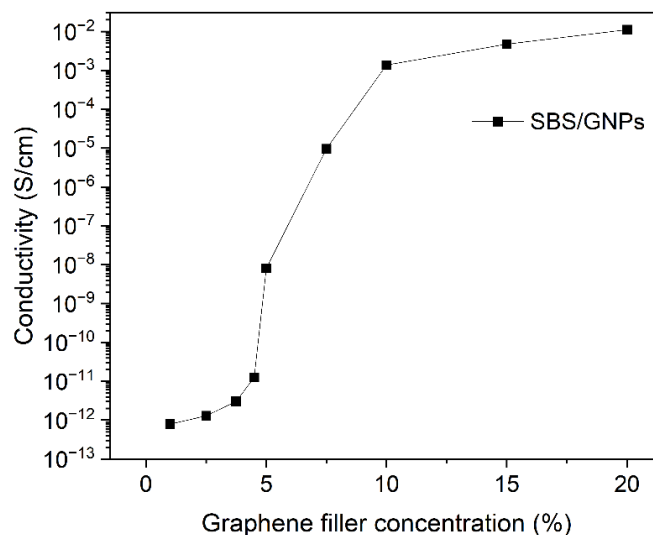


Figure 9: Percolation curve - Dependence of the electrical conductivity of SBS/GNPs on graphene concentrations. The lines connecting points serve only as a guide for eyes [RS3]

8.6.4 Response and selectivity of the sensor

The sensors were prepared from the selected material with a filler mass concentration of 7.5 % in the SBS/GNPs nanocomposite and tested against vapours of ethanol, acetone, toluene, and heptane. Examples of sensor responses to each of the tested vapours recorded for ten on/off cycles are plotted in Figure 10. Relative response to water was added too. [RS3]

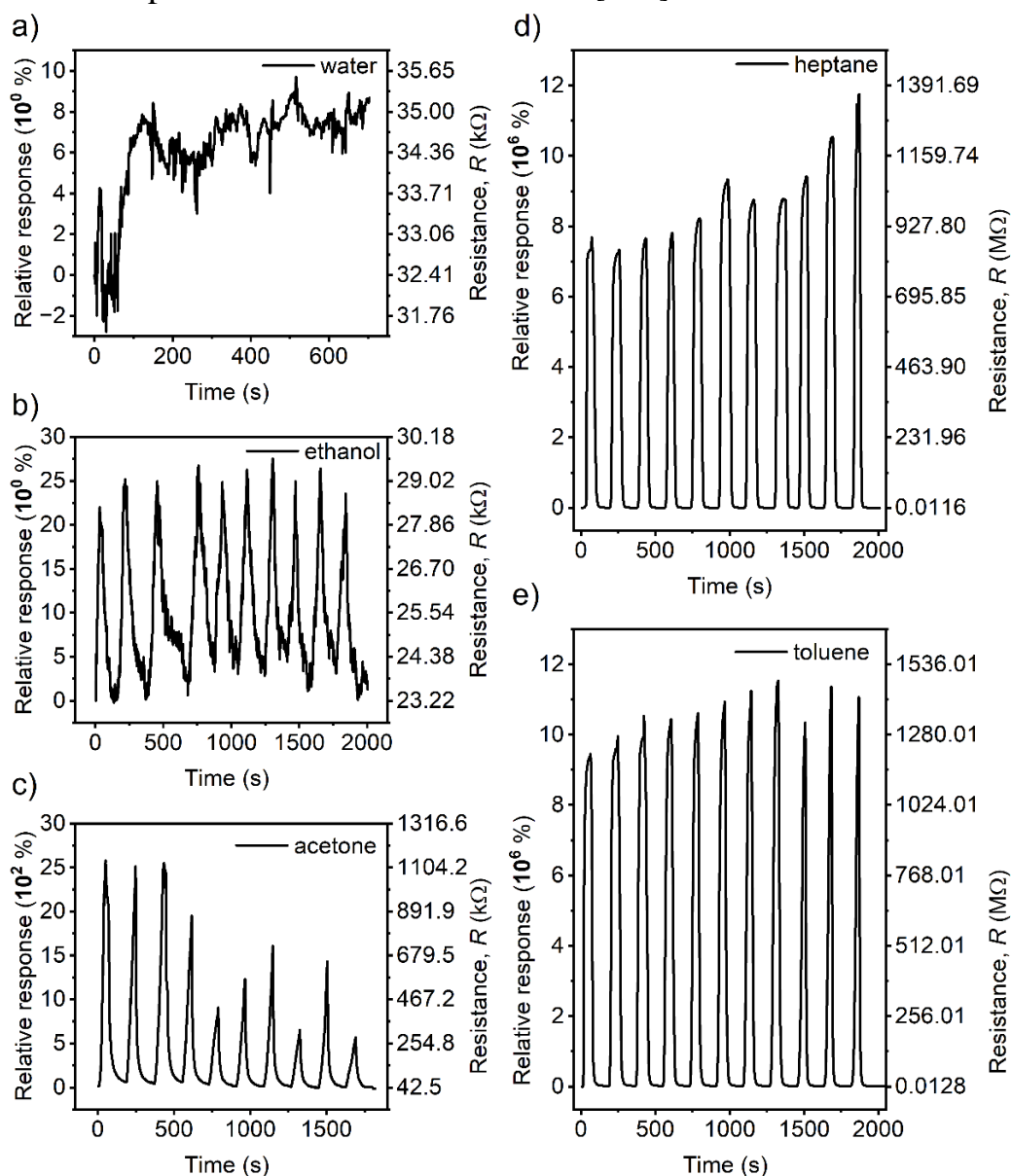


Figure 10 - Graphs of the sensor resistance (R) responses and relative responses of the SBS/GNPs sensor during the absorption/desorption cyclic phase for saturated vapours of all solvents, namely a) water, b) ethanol, c) acetone, d) heptane and e) toluene. Note the y-scales of the graphs – the units are $k\Omega$ for water, ethanol, and acetone, whereas the graphs recorded for toluene and heptane use $M\Omega$, as the sensor resistance changes are very large. The same scales apply for Relative response ($\Delta R/R_0$) expressed in % starting from units 10^0 , hundreds 10^2 up to millions 10^6 . [RS3]

Figure 10 a) shows the reaction of the sensor to relative humidity change from 40 % in the thermostatic box to 100 % in the testing flask. There was no significant response to the cycling, therefore we concluded that water has no or negligible role in sensing at given conditions. Then, the other VOCs were tested. The adsorption/desorption cycles yielded the typical shape of the response curves illustrating the giant relative response of sensors to some of the tested VOCs reaching up to millions of %, which in terms of electrical resistance represents a change from several tens of k Ω to several G Ω . It must be noted on account of the presented data that the testing apparatus and the method are elementary, and these measurements represent a pioneering study which will be more elaborated in further detailed research.

The observed highest R_{max}/R_0 and rounded average R_{max}/R_0 values are summarised in Table 4. The highest maximum relative response was recorded for toluene and heptane. In contrast, acetone vapours induced a small response, whereas ethanol vapours generated only little changes in the resistance.

Table 4 also summarises the response time (t_{90}) necessary for the sensor to reach 90 % of the maximum signal in the on phase of the cycle and the recovery time (t_{10}) necessary for the sensor to reach 10 % of the preceding maximum response in the off phase of the cycle. The values were read from the graphs in Figure 10 and are presented as average values with standard deviations. The values were obtained for the tested VOCs while water has no significant response.

Table 5 summarises the selectivity ($\sigma_{1/2}$) of the sensor towards vapours of the tested VOCs. [RS3]

Table 4: Results of max. values $\Delta R/R_0$ of the sensor towards tested VOCs. The values of saturated vapour partial pressure at 25 °C are taken from the following references: a) [37], b) [38], c) [39], and d) [40]. [RS3]

VOC	p_0 (kPa)	Maximum R_{max}/R_0 (%)	Average R_{max}/R_0 (%)	t_{90} (s)	t_{10} (s)
ethanol ^a	7.870	26.8	23	48 ± 13	110 ± 50
acetone ^b	30.868	2580	1600	52 ± 9	24 ± 4
toluene ^c	3.8	11 500 000	10 000 000	31 ± 4	22 ± 2
heptane ^d	6.476	11 600 000	9 000 000	24 ± 5	20 ± 2

Table 5: The selectivity ($\sigma_{1/2}$) of the sensor towards tested VOCs. [RS3]

Gas (VOC) 1	Gas (VOC) 2			
	ethanol	acetone	toluene	heptane
ethanol	1	0.056	0.00000111	0.0000021
acetone	18	1	0.0000197	0.0000373
toluene	901 000	50 800	1	1.8
heptane	476 000	26 800	0.528	1

8.6.5 Sensing mechanism

As presumed in the introductory part, the mechanism imparting the giant sensitivity and selectivity to the SBS/GNPs sensors can be described in terms of polymer swelling due to the adsorption of VOC molecules and their interaction with the polymer matrix. Nevertheless, some other possible mechanisms need to be reconsidered, including the interaction of the VOC molecules with the filler particle network. [RS3]

Although empirical, the Hansen solubility parameter (HSP) pragmatic approach fits well in the framework of classical polymer solution theories and earned its recognition in the prediction of polymer solubility [41]. *Similia similibus solvuntur* refers to an old general rule in chemistry, which says that similar substances dissolve similar substances. Dissolution and swelling of polymers are governed by the similarity of the solvent and the solute in three relevant parameters describing the effect of the dispersion force (δ_D), the polar intermolecular force (δ_p), and the hydrogen bond (δ_H). These three HSP describe the three major contributions to cohesion energy and create a three-dimensional space where a point represents a solvent or solute. The common unit for these parameters is MPa^{1/2}. The square of the Euclidean distance, $(r_a)^2$, between two points in the HSP space describes the difference in cohesion energy per molar volume between these two components, which is used to assess their mutual ability to form a solution (miscibility, in other words). The empirical parameter is the interaction radius (r_0) which expresses the maximum energy difference allowing solubility of the compound in question. This radius is indeed a Euclidean distance and defines the best spherical approximation of the volume surrounding the solute point in the HSP space embracing experimentally estimated solvents, the so-called interaction sphere. It is also called a solubility sphere as it encompasses good solvents for polymers. In contrast, points lying outside the sphere shall not dissolve the solute. Some thermodynamically bad solvents or even good solvents may fall out of the sphere as the estimation of its radius is based on statistics. Nevertheless, points representing such solvents will not be far from the sphere's surface. The relative energy difference (*RED*) used to predict the solubility of a polymer in a solvent is dimension less and defined as

$$RED = \frac{r_a}{r_0} \quad (7)$$

$$(r_a)^2 = 4(\delta_{D,pol} - \delta_{D,sol})^2 + (\delta_{p,pol} - \delta_{p,sol})^2 + (\delta_{H,pol} - \delta_{H,sol})^2 \quad (8)$$

The lower indexes “pol” and “sol” stand for polymer and solvent, respectively. Note that the lowercase symbol “*r*” is used here for the radius instead of the commonly used symbol “*R*” to avoid confusion with the electrical resistance.

The biphasic SBS co-polymer matrix in the nanocomposite can be treated as a combination of two model polymers PS and PB. Table 6 summarises the tabulated HSP of tested VOCs and the model polymers, interaction radii of PS and PB and

RED calculations. A *RED* value lower than 1 indicates the high miscibility of the VOC in the polymer in question. Ethanol and acetone have values of *RED* higher than 1, correlating to the observed small sensitivity response. Nevertheless, the acetone/ethanol selectivity value is 25, ascribed to the differences in their *RED* values calculated for both polymer phases. Indeed, neither PS nor PB dissolves in ethanol, whereas acetone nearly approaches the limit of good solubility defined by $RED = 1$ for both polymers, thus providing limited solubility for SBS. A more complicated pattern can be seen for toluene and heptane. Toluene is the best-scoring solvent for both polymers and dissolves PS, PB, and the SBS co-polymer. In contrast, heptane does not dissolve PS, whereas it is a good solvent for PB. The relative response and selectivity of the sensor towards vapours of all tested VOCs follow the order of the corresponding HSP values. Water is considered in Table 6 to complete the picture. Indeed, it causes no significant sensor response, which correlates with its high *RED* and the fact that either PS or PB are insoluble in water and do not swell. On the other hand, it must be emphasized that water is an *enfant terrible* in the HSP approach. The parameters for a single water molecule derived from the energy of vaporization of water at 25 °C [41], were used in this table as this may correspond to the very low concentration of the molecules in the polymer or to the gaseous phase at best. [RS3]

Table 6: The HSP and r_0 values [41], calculated r_a values, and calculated *RED* values between PS, PB, and tested VOCs and water. [RS3]

Polymers & solvents	HSP values			r_0 (MPa ^{1/2})	r_a (MPa ^{1/2})	<i>RED</i> (-)
	δ_D (MPa ^{1/2})	δ_p (MPa ^{1/2})	δ_H (MPa ^{1/2})			
PS	22.3	5.8	4.3	12.7	-	-
water	15.5	16.0	42.3	-	41.63	3.28
ethanol	15.8	8.8	19.4	-	20.15	1.59
acetone	15.5	10.4	7.0	-	14.61	1.15
toluene	18.0	1.4	2.0	-	9.93	0.78
heptane	15.3	0	0	-	15.75	1.24
PB	17.5	2.3	3.4	6.5	-	-
water	15.5	16.0	42.3	-	41.44	6.38
ethanol	15.8	8.8	19.4	-	17.6	2.71
acetone	15.5	10.4	7	-	9.72	1.5
toluene	18	1.4	2	-	1.94	0.3
heptane	15.3	0	0	-	6.02	0.93

The HSP plot in Figure 11 offers a much more understandable picture, as it visualises the numbers in their geometrical meaning using the main advantage of the HSP approach. There are two solubility spheres, the larger in cyan, corresponding to PS with r_0 value of 12.7 MPa^{1/2}, and the smaller in magenta,

corresponding to PB with r_0 value of $6.5 \text{ MPa}^{1/2}$. The two spheres have an intersecting volume, defining an HSP space for common solvents. Nevertheless, the volumes not included in the intersection are significantly larger, encompassing HSP values specific for either PS or PB components, which indicates their different solubility behaviour. Thus, the union of the two balls represents a model of the two structural components in the SBS co-polymer. The ethanol point is far from the surface, does not dissolve the polymers, and induces the sensor's smallest response. The acetone point is outside the union volume also, but still very close to both spheres and gives a much higher signal. The toluene point is inside the two spheres' intersection and dissolves both polymer components well. The heptane point is only inside the solubility sphere of PB and is not included in the one of PS. The solubility is the main factor in the sensor's large sensitivity to toluene and giant sensitivity to heptane, whereas the mutual heptane/toluene selectivity can be ascribed to the difference in solubilities of individual components. [RS3]

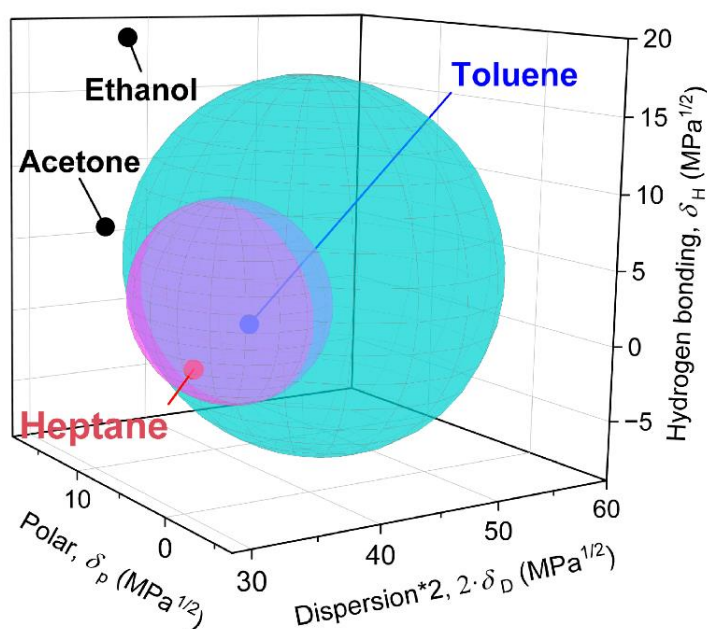


Figure 11 – HSP plot for tested VOCs and solubility spheres of the two components of SBS co-polymer. Water is not plotted as this is an unnecessary outlier and would deform the scale suitable for reading the picture. Based on the data from Table 13 and references therein. [RS3]

It must be stressed that the used SBS block co-polymer contains only 30 wt.% of styrene content. It is a thermoplastic elastomer with a major continuous flexible PB phase, whereas the discontinuous PS domains create rigid crosslinking points. Toluene swells both phases of the sensor's SBS polymer matrix well, which is responsible for the high sensitivity towards it. However, at the same time, it causes softening, plastification and relaxation of the whole material, including the relaxation of the GNPs filler percolating network. Therefore, the increasing distance between the filler particles is considered the primary sensing response

mechanism, whereas the filler network relaxation may work in the opposite direction. Heptane does not dissolve PS, but it dissolves PB well. Therefore, the PB continuous phase becomes readily swollen when absorbing heptane vapours, while the PS domains are less affected. Both solvents efficiently swell the material and the volume increase of the material due to swelling will induce stress rather than relaxation. This will not only depreciate the tunnelling contacts between the filler particles due to increasing interparticle distance, but the filler network can also be deformed. Such network disruptions can be especially expected at the interfaces between PB's and PS's phase domains due to their different degrees of swelling by the tested solvent. Moreover, the stress due to the volume expansion of the matrix can cause deformations of GNPs sheets not only at the phase interfaces but also in the volume of phases. Bending deformations of graphene sheets will decrease their conductivity, thus contributing to the overall increase of the SBS/GNPs nanocomposite giant resistivity response when exposed to heptane and toluene vapours. [RS3]

Table 7 summarises the values of relevant parameters and results of calculations in the same fashion as Table 6. First, the interaction of graphene and polymer matrices has to be evaluated. It seems the PB is closer than PS to the surface of the graphene's solubility sphere indicating better (yet still not good) dispersibility and, more generally, a greater affinity between the polymer and the filler than in the case of PS. The stronger interaction between PB and the graphene sheets can be due to the contribution of dispersion forces, as the δ_D value of PB is much closer to graphene than the δ_D value of PS. We also know from the previous considerations that heptane has excellent and probably selective interaction with the PB phase. On the other hand, the *RED* value for the graphene–heptane pair suggest the worst solubility mainly due to a large discrepancy in the effects of intermolecular forces and hydrogen bond interactions. In contrast, toluene does not provide such specificity. Thus, the co-occurrence of these two opposite mechanisms also contributes to the observed giant response and selectivity of the SBS/GNPs sensor. [RS3]

Table 7: The HSP and r_0 values [41–43], calculated r_a values, and *RED* values between graphene and PS, PB, and tested VOCs. [RS3]

Polymers & solvents	HSP values			r_0 (MPa ^{1/2})	r_a (MPa ^{1/2})	<i>RED</i> (-)
	δ_D (MPa ^{1/2})	δ_p (MPa ^{1/2})	δ_H (MPa ^{1/2})			
graphene	18.0	9.3	7.7	6.5	-	-
PS	22.3	5.8	4.3	-	9.89	1.52
PB	17.5	2.3	3.4	-	8.28	1.27
Ethanol	15.8	8.8	19.4	-	12.51	1.92
Acetone	15.5	10.4	7.0	-	5.17	0.80
Toluene	18.0	1.4	2.0	-	9.74	1.50
Heptane	15.3	0	0	-	13.23	2.04

The large difference between *RED* values of ethanol and acetone in Table 7 is also worth of attention. The difference in affinity of acetone and ethanol to graphene may provide an additional explanation for the mechanism of the sensor's selectivity towards these two VOCs. As it was shown, acetone is better than ethanol in swelling the co-polymer matrix components, although the poor solubility in the matrix is still the main factor limiting the sensor's sensitivity toward both of them. Nonetheless, the *RED* of acetone to graphene is the best among all other components. As a result, the acetone molecules may preferentially be adsorbed on the graphene sheets if penetrated through the matrix. Then, they can contribute selectively to a matrix volume increase localised in the filler particles' intimate proximity, which further impedes the tunnelling charge transport, additionally increasing the sensor's response to acetone. [RS3]

The observed effects of 100 % humidity or nearly saturated water vapour pressure are not intrinsic. The sensor has neither a positive nor a negative response towards water vapours, including saturated vapours, as shown in Figure 10 a). There is no simple summation of the signal contributions. Indeed, the water does not interact with the co-polymer matrix volume regarding swelling, as discussed above. Hence, an interaction on the nanocomposite surface must be considered. It can be assumed that when the relative humidity approaches 100 %, water may be adsorbed or even condensed on the rough surface of the nanocomposite. Such polar barrier may be responsible for the slightly diminished response towards hydrophobic VOCs, whereas its effect on the polar VOCs may be more pronounced as they are miscible with water, and local equilibria may influence the process of adsorption and desorption of the polar molecules. Whereas the signal is slightly decreased for hydrophobic molecules and remains stable, it is largely suppressed for the polar substances and shows marks of a decrease with time, which, paradoxically, contribute to the selectivity enhancement. [RS3]

To emphasise finally, both main advantages of HSP, i.e., simplicity, explanatory and predictive power, were also proven in this study of a non-trivial graphene block co-polymer matrix nanocomposite-based sensor device, thus extending the applicability of this approach to the field of sensors. Although further systematic and more elaborated characterisation studies must be performed, we believe it is legitimate to coin the term Hansen solubility parameters-based sensors for the class of sensors working on the sensing principles demonstrated in this study which may become game-changing in the future. It is not only description and explanation that is possible now, but a rational design of new sensors of this class is enabled using the discovered pieces of the sensing mechanism and knowledge of factors playing roles in the solvent–polymer–filler interactions. [RS3]

9. CONCLUSIONS

This work aimed to facilitate the detection of volatile organic compounds (VOCs) by research and development of a new nanocomposite sensor based on carbon filler in a polymer matrix. Ethanol, acetone, toluene and heptane have been selected as representative VOCs according to their differences in polarity and hydrophobicity. A suitable combination of the filler and matrix can enhance the sensitivity and selectivity of the sensor prepared by solution casting methods.

The results of the initial heuristics confirmed MWCNTs as the best candidate in comparison with carbon black and carbon fibres. Preliminary screening of polymer matrices excluded thermoplastic polymers (PS and PMMA) whereas thermoplastic elastomer matrices (TPU, EOC and SIS) were found suitable. These polymers are soluble and easily processable and prepared sensors proved that the composite could detect saturated organic vapours, which in turn characteristically alter their electrical resistance. The sensor based on the MWCNT filler and the styrene-isoprene-styrene copolymer has the highest sensitivity for the vapour of heptane, followed by nearly two times lower sensitivity to toluene. A moderate response can be observed for vapour of acetone, and the lowest sensitivity is experienced for the vapour of ethanol. [RS1]

According to the preliminary understanding, the choice of polymer matrix imparts the selectivity to the sensor due to differences in similarity of the tested VOCs with the structure of the polymer matrix. Moreover, the gas sensor samples developed at this stage of the research were small and production costs were low. It could be practically used as a part of a universal device for identification of organic solvent vapours, so called "electronic nose" that has been demonstrated with integrated electronic device indicating the VOC component. Another direction of practical use of the sensor was demonstrated with the microstrip antenna sensing device. [RS2]

The efforts to improve the nanocomposite sensor led to another explorative research activities. First, the graphene filler in form of graphene nanoplatelets (GNPs) was introduced to the experimental design. The nanocomposites based on GNPs and elastomer matrix (first SIS, then SBS) resulted in best percolation curves allowing a more sophisticated choice of the filler concentration for the nanocomposite transducing layer in the sensor. Another experimental approach how to enhance the sensing film properties was based in air plasma surface modification. Although there were good indications for this approach from our collaborating institute in Slovenia, the atmospheric plasma treatment experiments did not lead in satisfying results. The main prediction and motivation were to decrease the electrical resistance of the measuring layer and simultaneously increase the electrical conductivity of the sensors. The effect of the treatment on the sample resistance was very fast, however, the modified properties were highly unstable. Another way how to improve the sensor properties was focused on the thin film preparing technique. The work was started with the full awareness of the

disadvantages of manual dip coating methods; however, it was the easiest and fastest entrance to the preliminary stage of the research. In spite of the relatively poor thickness reproducibility, repeatability, and homogeneity of the layers, the initial heuristics provided valuable results. Nevertheless, automated dip coating and spin coating were examined as the next steps aimed at improving the preparation of the composite layer. The automatic dipping allowed preparation of samples with the thickness characterised by the 30 % relative standard deviation. The spin coating allowed to prepare samples of thickness within ± 10 % standard deviation.

Using all these prerequisites, it was possible to prepare a chemiresistive VOC sensor with a giant sensitivity and selectivity using electrically percolating SBS/GNPs nanocomposite as a sensitive layer deposited by spin coating on a copper IDE patterned substrate. Three general rules of successful material selection, material design and sensor construction were applied. As a result, the sensor provided highly selective responses to saturated vapours of representative VOCs differing in sensitivity values by orders of magnitude, i.e. average maximum sensitivity (R_{\max}/R_0) for ethanol 23 %, acetone 1 600 %, up to the giant value for n-heptane 9 000 000 % and toluene 10 000 000 %, which corresponds to resistance response change from several tens of k Ω to several G Ω . Although humidity somewhat decreases the response of the sensor to the tested gases at room temperature, it improves the selectivity of the sensor, enhancing the resolution between hydrocarbons (represented by aliphatic heptane and aromatic toluene) and polar organic compounds (represented by acetone and ethanol). [RS3] The GNPs filled nanocomposite material with SBS co-polymer matrix represents a non-trivial example of graphene or any other nano-carbonaceous filler-based polymer matrix composite material for constructing chemiresistive sensors. The complex sensing mechanism of this kind of sensor is based on non-bonding intermolecular interactions. Therefore, the sensor response is governed by several effects, some of which can be synergic or antagonistic and manifested depending upon a proper sensor's material selection, tuning electrical properties using percolation theory, and construction design. The key factors and their intriguing roles in the sensing mechanism were described and explained in terms of the Hansen solubility parameters approach, providing simple and explanatory sufficient insight into the involved intermolecular interactions. Moreover, based on the clarified sensing principles and knowing factors playing roles in the solvent-polymer-filler interactions, a rational design of new sensors is enabled due to the HSP approach predictive power in future. Thus, a new class of sensors is announced under the name "Hansen solubility parameters-based" (HSP-based) sensors. [RS3]

10. CONTRIBUTION TO SCIENCE AND PRAXIS

Besides the generalisation of all the experience gathered during the first parts of the experimental studies, the most important contribution can be drawn from the original introduction of the HSP approach to sensor science and technology and the future vision that is opened by this work.

Although the HSP approach is based primarily on empirical facts of experimental solubility observations, it also provides a scientifically sound insight into the nature of non-bonding intermolecular interactions. Both main advantages of HSP, i.e. simplicity, explanatory and predictive power, were proven in this study of a non-trivial graphene block co-polymer matrix nanocomposite-based sensor device, extending thus newly the applicability of this approach to the field of sensors. It is legitimate to coin the term Hansen solubility parameters-based sensors for the class of sensors working on the sensing principles demonstrated in this study, which may become game-changing in future. It is not only description and explanation that is possible now, but a rational design of new sensors of this class is enabled using the discovered sensing mechanism and knowledge of factors playing roles in the solvent-polymer-filler interactions.

General lessons from experience presented in this work can be summarised. First, the choice of materials is crucial to the sensor's design. A composite or nanocomposite consists of at least one polymer matrix and a particulate filler. If a homopolymer is chosen in the simplest example, the response is driven by the ability of the matrix to adsorb the tested VOC's molecules and swell. Then, the selectivity will be predictable based on HSP parameters and the *RED* as a single parameter, and the mechanism will be the matrix expansion, worsening the tunnelling transport mechanism combined eventually with the deformation of filler particles, which might be complicated by an antagonistic effect of the relaxation of the filler network in a softened matrix.

Specific interaction of the filler with the tested VOCs can improve the selectivity if this is the case. Although only one type of GNPs filler was used in the presented study, exceptional acetone affinity to graphene demonstrated that a specific interaction of the VOC with the filler can provide another contribution to the selectivity. The simultaneous use of various fillers can offer a higher chance for selective interaction between the analyte and each type of used filler. For example, various types of surface-modified carbonaceous filler could be used, or combinations of carbon-based fillers with other elemental compositions (e.g. C_3N_4 or MO_x) are encouraged to enhance the selectivity of the sensor.

To achieve a non-trivial response behaviour of the sensor, a multiphase composition of the polymer matrix is suggested. Using two or more polymer components with sufficiently differing solubility spheres in the HSP space can provide a selectively responding multiphase system. Depending upon the miscibility and compatibility of the polymers, which can also be assessed using the HSP approach, polymer phases of different compositions can be formed

containing a percolating filler network. Mixing homopolymers offers many possible combinations, especially mixtures of immiscible polymers with various degrees of compatibility, which may be further modified with compatibilisers. On the other hand, the resulting structure and phase morphology will heavily depend on the mixing and film preparation procedures. The resulting phase morphology can also be varied in terms of continuity, discontinuity, or co/continuity of phases. Moreover, the dispersion and distribution of the filler can be different in each phase. As a result, a multiphase system with dispersed filler particles throughout the matrix can selectively respond to various VOCs due to their different interactions with individual phases. The strongest effect is expected at the phase interfaces where a mismatching in the swelling volume expansion of the neighbouring phases can dramatically alter the interphase connectivity of the filler network. This strategy offers a broad selectivity, but the control of the fabrication process may become an intriguing task. Therefore, it is alternatively suggested to choose a block co-polymer system where the dispersion and distribution of phases are assured simply by the fact of the given molecular architecture. SBS was chosen to pave this more manageable way, providing two polymer phases that enabled the observation of principles of all aforementioned effects.

Further, applying the filler concentration choice rule was proven effective. The right composition is to be chosen between the percolation threshold and the saturation part of the percolation curve. Such option can be generally advised for the material design of HSP-based (nano)composite sensors, as it provides a combination of high sensitivity with an extensive resistivity range available for the response.

Finally, a few remarks on thickness can be made. Indeed, the transducing nanocomposite layer should be thick enough to allow the filler to be well dispersed and spatially distributed to create an electrically conductive network by the interconnected filler particles of the kind in question. On the other hand, the transducing layer should be thin enough to provide a fast sensor response and avoid undesirable thickness-related effects. In an ideal case, the filler shape and the process should allow a flat (2D) structure to form with good dispersion and distribution of the filler. An interesting idea would also be a combination of a high aspect ratio filler (such as graphene or carbon nanotubes) with carbon black or carbon dots, modifying the conductivity.

In this vision, the original HSP-based approach to sensor design opens a window for relatively easy and cheap production of multiple kinds of sensors by varying materials according to the above-mentioned simple principles in the future. A set of such sensors of different selectivity might be once combined into a matrix of small-size devices, preparing thus a not only so-called but a real „electrical nose”.

REFERENCES

Author's publications

- [RS1] SLOBODIAN, Rostislav, Robert OLEJNIK, Jiri MATYAS and Petr SLOBODIAN. THE SENSING PROPERTIES OF CARBON NANOTUBE FILLED COPOLYMERS FOR VOC VAPORS DETECTION. In: 12TH INTERNATIONAL CONFERENCE ON NANOMATERIALS - RESEARCH & APPLICATION (NANOCON 2020) [online]. 2021, p. 63–67. ISBN 978-80-87294-98-7. Available at: doi:10.37904/nanocon.2020.3695
- [RS2] SLOBODIAN, Petr, Pavel RIHA, Robert OLEJNIK, Jiri MATYAS and Rostislav SLOBODIAN. Microstrip Resonant Sensor for Differentiation of Components in Vapor Mixtures. *SENSORS* [online]. 2021, **21**(1). Available at: doi:10.3390/s21010298
- [RS3] SLOBODIAN, Rostislav, Robert OLEJNIK, David John DMONTE, Jakub SEVCIK, Jiri MATYAS, Marek JURCA, R. Blessy PRICILLA, Barbora HANULIKOVA, Petr SLOBODIAN and Ivo KURITKA. Giant Response and Selectivity of Hansen Solubility Parameters-Based Graphene-SBS Co-Polymer Matrix Composite Room Temperature Sensor to Organic Vapours. *Polymers* 2024, Vol. **16**, Page 309 [online]. 2024, 16(3), 309. ISSN 2073-4360. Available at: doi:10.3390/POLYM16030309

Other references

- [1] ASHBY, Michael F., Paulo J. FERREIRA and Daniel L. SCHODEK. *Nanomaterials, nanotechnologies and design: An introduction for engineers and architects* [online]. 2009. ISSN 0009-4978. Available at: doi:10.5860/choice.47-2023
- [2] KOO, Joseph. *Polymer Nanocomposites: Processing, Characterization, And Applications (Mcgraw-Hill Nanoscience and Technology Series)* [online]. B.m.: McGraw-Hill Professional, 2006. ISBN 0071458212. Available at: <http://www.amazon.com/Polymer-Nanocomposites-Characterization-Applications-Mcgraw-Hill/dp/0071458212>
- [3] MITTAL, Vikas. *Polymer Nanotube Nanocomposites: Synthesis, Properties, and Applications* [online]. 2010. Available at: doi:10.1002/9780470905647
- [4] ŠPITALSKÝ, Zdenko, Ján KRATOCHVÍLA, Katarína CSOMOROVÁ, Igor KRUPA, Manuel P.F. GRAÇA and Luis C. COSTA. Mechanical and Electrical Properties of Styrene-Isoprene-Styrene Copolymer Doped with Expanded Graphite Nanoplatelets. *Journal of Nanomaterials* [online]. 2015, **2015**. ISSN 16874129. Available at: doi:10.1155/2015/168485
- [5] *Polymer Database* [online]. 2023. Available at: https://polymerdatabase.com/polymer_classes/Polyurethane_type.html
- [6] *Thermoplastic Polyurethane | Covestro AG* [online]. Available at: <https://solutions.covestro.com/materials/thermoplastic-polyurethane>
- [7] *MATWEB: thermoplastic polyurethanes* [online]. Available at: <https://www.matweb.com/search/datasheet.aspx?matguid=c99615b3972645a8994c1b2f69a3656e&ckck=1>
- [8] SEDLÁKOVÁ, Zuzana, Gabriele CLARIZIA, Paola BERNARDO, Johannes Carolus JANSEN, Petr SLOBODIAN, Petr SVOBODA, Magda KÁRÁSZOVÁ, Karel FRIESS and Pavel IZAK. Carbon Nanotube- and Carbon Fiber-Reinforcement of Ethylene-Octene Copolymer Membranes for Gas and Vapor Separation. *Membranes 2014, Vol. 4, Pages 20-39* [online]. 2014, **4**(1), 20–39. ISSN 2077-0375. Available at: doi:10.3390/MEMBRANES4010020

- [9] TESARIKOVA, Alice, Dagmar MERINSKA, Jiri KALOUS and Petr SVOBODA. Ethylene-Octene Copolymers/Organoclay Nanocomposites: Preparation and Properties. *Journal of Nanomaterials* [online]. 2016, **2016**. ISSN 16874129. Available at: doi:10.1155/2016/6014064
- [10] MATWEB: *thermoplastic elastomers* [online]. Available at: <https://www.matweb.com/search/datasheet.aspx?MatGUID=04edcf2cb10d40b5aa414f995f6904f8>
- [11] *Polymer Database* [online]. Available at: <https://polymerdatabase.com/Elastomers/SBS-SIS.html>
- [12] *Merck: Sigma Aldrich* [online]. Available at: <https://www.sigmaaldrich.com/CZ/en/product/aldrich/432490>
- [13] SANDERS, Wesley Crowell. *Basic Principles of Nanotechnology*. B.m.: CRC Press – Taylor & Francis, 2018. ISBN 978-1-138-48361-3.
- [14] CHUNG, Deborah D L. *Carbon materials: science and applications*. B.m.: World Scientific Publishing Co Pte Ltd., 2019. ISBN 9789813221901.
- [15] PRASEK, Jan, Jana DRBOHLAVOVA, Jana CHOMOUCKA, Jaromir HUBALEK, Ondrej JASEK, Vojtech ADAM and Rene KIZEK. Methods for carbon nanotubes synthesis—review. *Journal of Materials Chemistry* [online]. 2011, **21**(40), 15872–15884. ISSN 1364-5501. Available at: doi:10.1039/C1JM12254A
- [16] O'CONNELL, Michael J. *Carbon Nanotubes Properties and Applications*. B.m.: CRC Press – Taylor & Francis, 2018. ISBN 9781315222127.
- [17] KATSNELSON, Mikhail I. *Graphene | Properties, Uses & Structure | Britannica* [online]. Available at: <https://www.britannica.com/science/graphene>
- [18] CLYNE, T. W., Derek HULL and MATERIALS RESEARCH SOCIETY. An introduction to composite materials [online]. no date, 345. Available at: https://books.google.com/books/about/An_Introduction_to_Composite_Materials.html?hl=cs&id=4oKWDwAAQBAJ
- [19] VILČÁKOVÁ, Jarmila and UNIVERZITA TOMÁŠE BATI VE ZLÍNĚ. TECHNOLOGICKÁ FAKULTA. Elektrické a magnetické vlastnosti polymerních kompozitů = Electrical and magnetic properties of polymer composites : teze habilitační práce [online]. 2007. Available at: https://books.google.com/books/about/Elektrick%C3%A9_a_magnetick%C3%A9_vlastnosti_pol.html?hl=cs&id=jxiYtwAACAAJ
- [20] KICKELBICK, Guido and EDITOR. *Hybrid Materials: Synthesis, Characterization, and Applications*. 2007.
- [21] MA, Peng Cheng and Jang Kyo KIM. Carbon nanotubes for polymer reinforcement. *Carbon Nanotubes for Polymer Reinforcement* [online]. 2011, 1–193. Available at: doi:10.1201/B10795/CARBON-NANOTUBES-POLYMER-REINFORCEMENT-PENG-CHENG-MA-JANG-KYO-KIM
- [22] ALEXANDRE, Michael and Philippe DUBOIS. Polymer-layered silicate nanocomposites: preparation, properties and uses of a new class of materials. *Materials Science and Engineering: R: Reports* [online]. 2000, **28**(1–2), 1–63. ISSN 0927-796X. Available at: doi:10.1016/S0927-796X(00)00012-7
- [23] WILSON, Jon. Sensor Technology Handbook - 1st Edition. *Elsevier* [online]. 2005, 1–704. Available at: <https://www.elsevier.com/books/sensor-technology-handbook/wilson/978-0-7506-7729-5>
- [24] FRADEN, Jacob. Handbook of Modern Sensors - Physics, Designs, and Applications. *Springer Science* [online]. 2010. Available at: doi:10.1007/978-1-4419-6466-3
- [25] SLOBODIAN, P., P. RIHA and R. OLEJNIK. Electromechanical sensors based on carbon nanotube networks and their polymer composites. *Springer - Lecture Notes in*

- Electrical Engineering* [online]. 2011, **83 LNEE**(New Developments and Applications in Sensing Technology), 233–251. ISSN 18761100. Available at: doi:10.1007/978-3-642-17943-3_12/COVER
- [26] KUCHAKOVA, Iryna, Maria Daniela IONITA, Andrada IONITA EUSEBIU-ROSINI AND LAZEA-STOYANOVA, Simona BRAJNICOV, Bogdana MITU, Gheorghe DINESCU, Mike DE VRIEZE, Uros CVELBAR, Andrea ZILLE, Christophe LEYS and Anton YU NIKIFOROV. Atmospheric Pressure Plasma Deposition of Organosilicon Thin Films by Direct Current and Radio-frequency Plasma Jets. *MATERIALS* [online]. 2020, **13**(6). Available at: doi:10.3390/ma13061296
- [27] CVELBAR, U, D VUJOSEVIC, Z VRATNICA and M MOZETIC. The influence of substrate material on bacteria sterilization in an oxygen plasma glow discharge. *JOURNAL OF PHYSICS D-APPLIED PHYSICS* [online]. 2006, **39**(16), 3487–3493. ISSN 0022-3727. Available at: doi:10.1088/0022-3727/39/16/S06
- [28] GEIM, A. K. and K. S. NOVOSELOV. The rise of graphene. *Nature Materials* 2007 6:3 [online]. 2007, **6**(3), 183–191. ISSN 1476-4660. Available at: doi:10.1038/nmat1849
- [29] SCHEDIN, F, A K GEIM, S V MOROZOV, E W HILL, P BLAKE, M I KATSNELSON and K S NOVOSELOV. Detection of individual gas molecules adsorbed on graphene. *NATURE MATERIALS* [online]. 2007, **6**(9), 652–655. ISSN 1476-1122. Available at: doi:10.1038/nmat1967
- [30] SCRIVEN, L. E. Physics and Applications of DIP Coating and Spin Coating. *MRS Proceedings* [online]. 1988, **121**(1), 717–729. ISSN 0272-9172. Available at: doi:10.1557/PROC-121-717/METRICS
- [31] BORNSIDE, David E, Christopher W MACOSKO and L E SCRIVEN. MODELING OF SPIN COATING. *Journal of imaging technology* [online]. 1987, **13**, 122–130. Available at: <https://api.semanticscholar.org/CorpusID:139001433>
- [32] JING, Zhao, Zhang GUANG-YU and Shi DONG-XIA. Review of graphene-based strain sensors. *CHINESE PHYSICS B* [online]. 2013, **22**(5). ISSN 1674-1056. Available at: doi:10.1088/1674-1056/22/5/057701
- [33] BENLIKAYA, Ruhan, Petr SLOBODIAN, Karel PROISL and Ilya CVELBAR UROS AND MOROZOV. Ascertaining the factors that influence the vapor sensor response: The entire case of MWCNT network sensor. *SENSORS AND ACTUATORS B-CHEMICAL* [online]. 2019, **283**, 478–486. ISSN 0925-4005. Available at: doi:10.1016/j.snb.2018.11.160
- [34] SANTHOSH, Neelakandan M, Aswathy VASUDEVAN, Andrea JUROV, Anja KORENT, Petr SLOBODIAN, Janez ZAVASNIK and Uros CVELBAR. Improving sensing properties of entangled carbon nanotube-based gas sensors by atmospheric plasma surface treatment. *MICROELECTRONIC ENGINEERING* [online]. 2020, **232**. ISSN 0167-9317. Available at: doi:10.1016/j.mee.2020.111403
- [35] STAUFFER, Dietrich and Ammon AHARONY. Introduction To Percolation Theory : Second Edition. *Introduction To Percolation Theory* [online]. 2018. Available at: doi:10.1201/9781315274386
- [36] ALAMUSI, Ning HU, Hisao FUKUNAGA, Satoshi ATOBE, Yaolu LIU and Jinhua LI. Piezoresistive Strain Sensors Made from Carbon Nanotubes Based Polymer Nanocomposites. *SENSORS* [online]. 2011, **11**(11), 10691–10723. Available at: doi:10.3390/s111110691
- [37] AMBROSE, D. and C. H.S. SPRAKE. Thermodynamic properties of organic oxygen compounds XXV. Vapour pressures and normal boiling temperatures of aliphatic alcohols. *The Journal of Chemical Thermodynamics* [online]. 1970, **2**(5), 631–645. ISSN 0021-9614. Available at: doi:10.1016/0021-9614(70)90038-8

- [38] AMBROSE, D., C. H.S. SPRAKE and R. TOWNSEND. Thermodynamic properties of organic oxygen compounds XXXIII. The vapour pressure of acetone. *The Journal of Chemical Thermodynamics* [online]. 1974, **6**(7), 693–700. ISSN 0021-9614. Available at: doi:10.1016/0021-9614(74)90119-0
- [39] BESLEY, L. M. and G. A. BOTTOMLEY. Vapour pressure of toluence from 273.15 to 298.15 K. *The Journal of Chemical Thermodynamics* [online]. 1974, **6**(6), 577–580. ISSN 0021-9614. Available at: doi:10.1016/0021-9614(74)90045-7
- [40] CARRUTH, G F and KOBAYASHI.R. VAPOR-PRESSURE OF NORMAL PARAFFINS ETHANE THROUGH N-DECANE FROM THEIR TRIPLE POINTS TO ABOUT 10 MM HG. *JOURNAL OF CHEMICAL AND ENGINEERING DATA* [online]. 1973, **18**(2), 115–126. ISSN 0021-9568. Available at: doi:10.1021/je60057a009
- [41] HANSEN, Charles M. Methods of characterization - surfaces. *Hansen Solubility Parameters: A Users Handbook, Second Edition* [online]. 2007, 113–123. Available at: doi:10.1201/9781420006834/HANSEN-SOLUBILITY-PARAMETERS-CHARLES-HANSEN
- [42] HERNANDEZ, Yenny, Mustafa LOTYA, David RICKARD, Shane D. BERGIN and Jonathan N COLEMAN. Measurement of Multicomponent Solubility Parameters for Graphene Facilitates Solvent Discovery. *LANGMUIR* [online]. 2010, **26**(5), 3208–3213. ISSN 0743-7463. Available at: doi:10.1021/la903188a
- [43] SALAVAGIONE, H J, J SHERWOOD, M DE BRUYN, G J BUDARIN V. L. AND ELLIS, J H CLARK and P S SHUTTLEWORTH. Identification of high performance solvents for the sustainable processing of graphene. *GREEN CHEMISTRY* [online]. 2017, **19**(11), 2550–2560. ISSN 1463-9262. Available at: doi:10.1039/c7gc00112f

LIST OF TABLES

Table 1: Compositions of tested samples for percolation threshold estimation A) for MWCNTs. Part B) shows the selected compositions for the preparation of testing Sensor specimens	20
Table 2: Results of max. values $\Delta R/R_0$ of composite materials (sensors) in a given solvent.....	22
Table 3: Compositions of tested samples for percolation threshold estimation A) for various concentrations of graphene. Part B) shows the selected compositions for the preparation of testing Sensor specimens.....	26
Table 4: Results of max. values $\Delta R/R_0$ of the sensor towards tested VOCs. The values of saturated vapour partial pressure at 25 °C are taken from the following references: a) [38], b) [39], c) [40], and d) [41].....	31
Table 5: The selectivity ($\sigma_{1/2}$) of the sensor towards tested VOCs.....	31
Table 6: The HSP and r_0 values [42], calculated r_a values, and calculated RED values between PS, PB, and tested VOCs and water.....	33
Table 7: The HSP and r_0 values [42, 42, 44], calculated r_a values, and RED values between graphene and PS, PB, and tested VOCs.....	35

LIST OF FIGURES

Figure 1: Experimental system for measuring resistance change.....	18
Figure 2: Percolation curve - Dependence of the electrical resistivity of MWCNT/copolymer composites on nanotube concentrations. The circles denote the given composites, which had the nearly identical resistivity of 300 Ωcm and hence were subsequently used for the comparison of the vapor effects.....	20
Figure 3: Graph of the sensitivity of the SIS/MWCNTs sensor during the absorption/desorption cyclic phase for vapours of all solvents.....	21
Figure 4: Graph of the sensitivity of the TPU/MWCNTs sensor during the absorption/desorption cyclic phase for vapours of all solvents.....	21
Figure 5: Graph of the sensitivity of the EOC/MWCNTs sensor during the absorption/desorption cyclic phase for vapours of all solvents.....	22
Figure 6: Maximal relative resistance changes (sensitivity) of the given MWCNTs/copolymer composite sensors and a pristine MWCNT network (buckypaper) upon exposure to the indicated chemical vapours. Composites are denoted in the figure as TPU, SIS and EOC, and pristine MWCNT networks as CNT. Data are depicted as means \pm SDs ($n = 5$).....	23
Figure 7: Device for evaluation of organic vapors, 1) during self-evaluation, 2) display of the evaluated solvent.....	24
Figure 8: Experimental system for measuring the resistance change response to saturated vapours of tested VOCs.....	28
Figure 9: Percolation curve - Dependence of the electrical conductivity of SIS/GNPs on graphene concentrations. The lines connecting points serve only as a guide for eyes.....	29
Figure 10: Graphs of the sensor resistance (R) responses and relative responses of the SBS/GNPs sensor during the absorption/desorption cyclic phase for saturated vapours of all solvents, namely a) water, b) ethanol, c) acetone, d) heptane and e) toluene. Note the y-scales of the graphs – the units are $k\Omega$ for water, ethanol, and acetone, whereas the graphs recorded for toluene and heptane use $M\Omega$, as the sensor resistance changes are very large. The same scales apply for Relative response ($\Delta R/R_0$) expressed in % starting from units 10^0 , hundreds 10^2 up to millions 10^6	30
Figure 11: HSP plot for tested VOCs and solubility spheres of the two components of SBS co-polymer. Water is not plotted as this is an unnecessary outlier and would deform the scale suitable for reading the picture. Based on the data from Table 13 and references therein.....	34

LIST OF SYMBOLS AND ACRONYMS

°C	Degree Celsius	nm	Nanometer
2D,3D	Two, Three dimensions/al	p_0	Partial pressure of VOCs
Ar	Argon	Pa	Pascal
C ₂ H ₂	Acetylene	PB	Polybutadiene
C ₂ H ₄	Ethylene	PCB	Printed circuit board
C ₃ N ₄	Graphitic carbon nitride	PMC	Polymer matrix composites
CB	Carbon black	PMMA	poly(methyl) methacrylate
CF	Carbon fibres	PN	Polymer nanocomposites
CMC	Ceramic matrix composites	PS	Polystyrene
CNTs	Carbon nanotubes	<i>R</i>	Resistance
Cu	Copper	<i>RED</i>	Relative energy difference
CVD	Chemical vapour deposition	rpm	Revolutions per minute
DWCNTs	Double wall carbon Nanotubes	s.	Second
EOC	Ethylene-octene-copolymer	SBS	Styrene-butadiene-styrene
FeCl ₃	Ferric chloride	SDNTs	Small-diameter carb. nanotubes
FTIR	FT Infrared microscopy	SEM	Scanning E. microscope
GNPs	Graphene nanoplatelets	SIS	Styrene-isoprene-styrene
GNWs	Graphene nanowalls	SWCNTs	Single-wall carbon nanotubes
h.	Hour/hours	TEM	Transmission E. microscope
He	Helium	TPU	Thermoplastic polyurethane
HSP	Hansen solubility parameters	VOCs	Volatile organic compounds
CH ₄	Methane	wt. %	Weight percent
IDE	Interdigitated electrode	ZnO	Zinc oxide
mm	Milimeter	μm	Micrometre
MMC	Metal matrix composites	$\sigma_{1/2}$	Selectivity pair of gasses
MO _x	Metal oxid	Ω	Ohm
MWCNTs	Multi-wall carbon nanotubes		

CURRICULUM VITAE



Personal information:

Name and surname: Rostislav Slobodian
Date of birth: 18. 02. 1992
Place of birth: Zlín, Czech Republic
Address: Hřebíčková 1320, Malenovice u
Zlína, 763 02
Nationality: Czech
E-mail: rslobodian@utb.cz, slobodian.r@seznam.cz
Phone: (+420) 605 354 610

Education:

2016– to date - Tomas Bata University in Zlín, Centre of Polymer Systems -
Ph.D. Study program: Nanomaterials and Nanotechnology, Field of
Study: Nanotechnology and Advanced Materials

2014 – 2016 - Tomas Bata University in Zlín, Faculty of Technology Study
program: Chemistry and Materials Technology Master's degree
study: Polymer Engineering
The theme of the master thesis: Detection of organic vapours by
using polymer composites/carbon allotropes with controlled
selectivity

2011 - 2014 Tomas Bata University in Zlín, Faculty of Technology Study
program: Chemistry and Materials Technology Bachelor's degree
study: Polymer Materials and Technology
The theme of the bachelor thesis: The system for monitoring of
motion based on randomly entangled carbon nanotubes embedded
in elastic polyurethane

2007 - 2011 Secondary Polytechnical School in Zlín Study program: Rubber
and Plastics Technology

Work experience:

 Rostislav Slobodian

LIST OF PROJECTS

RP/CPS/2020/006 Smart nanomaterials: from basics to application,
IGA/CPS/2021/002 Preparation and characterization of nanocomposite systems,
IGA/CPS/2020/003 Preparation and characterization of nanoparticles for advanced applications,
IGA/CPS/2019/007 Development and studies of conductive nanocomposite materials for electronic and electrotechnics applications,
IGA/CPS/2016/002 Thin polymer film with percolating carbon nanofiller network for detection of VOC.

LIST OF PUBLICATIONS

1. Slobodian, P.; Riha, P.; Olejnik, R.; Matyas, J.; Slobodian, R. Microstrip Resonant Sensor for Differentiation of Components in Vapor Mixtures. *Sensors*. 2021; 21(1):298. <https://doi.org/10.3390/s21010298>
2. Slobodian, R.; Olejnik, R.; Dmonte, D.J.; Sevcik, J.; Matyas, J.; Jurca, M.; Pricilla, R.B.; Hanulikova, B.; Slobodian, P.; Kuritka, I. Giant Response and Selectivity of Hansen Solubility Parameters-Based Graphene-SBS Co-Polymer Matrix Composite Room Temperature Sensor to Organic Vapours. *Polymers* 2024, 16, 309. <https://doi.org/10.3390/polym16030309>
3. Dmonte, D.J.; Bhardwaj, A.; Kavraz, P.; Slobodian, R.; Antos, J.; Sisman, O.; Galusek, D.; Fischer, T.; Mathur, S.; Kuritka, I. Detection of NH₃ gas using CrVO₄ nanoparticles, *Sensors and Actuators: B. Chemical*, (2024). <https://doi.org/10.1016/j.snb.2024.135380>

OVERVIEW OF OTHER ACTIVITIES

Conference proceedings:

1. Slobodian R., R. Olejník, J. Matyáš, I. Kuřitka and P. Slobodian. Graphene/elastomer nanocomposite VOC sensor with enhanced sensitivity and selectivity. 2nd World Graphene Technology Summit PHRONESIS, Miami 2022, USA, Book of abstracts: page 17 : Oral p.
2. Slobodian R. Selectivity enhancement of carbon nanotube composite sensor response to organic vapours by choice of the polymer matrix. 2nd International Meet & Expo on Nanotechnology NANOMEET 2022, Edinburgh 2022, Scotland (United Kingdom), Book of abstracts: pages 83-84 : Poster presentation + Contribution as Moderator
3. Slobodian R., R. Olejník, J. Matyáš, and P. Slobodian. The sensing properties of carbon nanotube filled copolymers for VOC vapours detection. 12th International Conference on Nanomaterials - Research & Application NANOCON, Brno 2020, Czech Republic, pages 63-67. ISBN 978-80-87294-98-7 : Conference proceedings
4. Slobodian, R., R. Olejník, P. Slobodian a J. Matyáš. Detekce par organických rozpouštědel pomocí vrstvy z polymerního kompozitu obsahujícího uhlíkové

nanotrubice. PLASTKO 2016 Conference proceedings, Zlín 2016, Czech Republic, str. 202-206. ISBN 978-80-7454-590-0 : Conference proceedings

Utility models:

1. Polymer compound for the production of profiles. Rostislav Slobodian, Radmila Horáková, David Hausner. ID 33915 – Utility model
2. Polymer compound based on secondary raw material. Rostislav Slobodian, David Hausner. ID 39256 – Utility model

Technical Internships:

Internship at Plastičářský klastr, z. s. (Zlín 2019) during 6 - 12/2019

Production cooperation:

Name of production project: Polymer compound for profile production (based on Utility model 33915) - cooperation with IKEA of Sweden, Älmhult (Sweden), serial production and sales of products: 9/2020 – 7/2022, including one month stay in Sweden 10/2019.

Significant trainings:

- Tire Academy – “fir for growth” 10-11/2017 (R.& D.), Continental AG, Hannover (Germany)
- Tire Academy – “learning initiative for tires” 3/2018 (R.& D.), Continental AG, Hannover (Germany)
- Project leadership: Lean Six Sigma – Green Belt – certificate holder (SC&C Partner, spol. s r.o., Brno 2018)
- Lean: project management (CE-PA, spol. s r.o, Zlín 2020)
- Academy controller – Controlling, forecasting, reporting, investment (CE-PA, spol. s r.o, Zlín 2020)
- Industry at EU level and chemical strategy for sustainability (Polymer Comply Europe, Brusel, Belgium), + Life Cycle Assessment - LCA study (VŠCHT Prague, prof. V. Kočí) 10-11/2021 – online sessions
- Business manager academy (UTB FaME, Zlín, 4-6 2022)
- PLASTKO 2022 – International professional conference, Czech Republic, Zlín, 21.-22. 9. 2022
- International Sales Meeting 2023 – Industrial chemistry (Setral Chemie GmbH, Garmisch, Germany) – 16.-19. 10. 2023
- OKS International Training 2023 – Tribology, Lubricants of Plastics and Elastomers (OKS Specialty Lubricants Ltd., Maisach, Germany) – 6.-8. 11. 2023

Awards:

- Top 10 Innovations for 2017 - Continental, s.r.o., Project title: Project for quality improvement of tread extruding
- The Price of the Director of the Polymer Centre, TBU Zlín, 2016 - for a master thesis on the topic: Detection of organic vapours by using polymer composites/carbon allotropes with controlled selectivity

Ing. Rostislav Slobodian, Ph.D.

Příprava a charakterizace nanokompozitních tenkých vrstev pro senzory par organických rozpouštědel

Preparation and characterization of nanocomposite thin films for sensors of organic solvent vapours

Doctoral Thesis Summary

Published by: Tomas Bata University in Zlín
nám. T. G. Masaryka 5555, 760 01 Zlín

Edition: published electronically

Typesetting by: Ing. Rostislav Slobodian, Ph.D.

This publication has not undergone any proofreading or editorial review.

Publication year: 2024

First Edition

ISBN 978-80-7678-263-1